



The Zwicky Transient Facility: Science Objectives

Matthew J. Graham¹, S. R. Kulkarni¹, Eric C. Bellm², Scott M. Adams¹, Cristina Barbarino³, Nadejda Blagorodnova¹, Dennis Bodewits^{4,5}, Bryce Bolin^{6,7,38}, Patrick R. Brady⁸, S. Bradley Cenko^{9,10}, Chan-Kao Chang (章展誥)¹¹, Michael W. Coughlin¹, Kishalay De¹, Gwendolyn Eadie^{2,6,12}, Tony L. Farnham⁴, Ulrich Feindt¹³, Anna Franckowiak¹⁴, Christoffer Fremling¹, Suvi Gezari^{4,9}, Shaon Ghosh⁸, Daniel A. Goldstein^{1,39}, V. Zach Golkhou^{6,12,s.40}, Ariel Goobar¹³, Anna Y. Q. Ho¹, Daniela Huppenkothen^{2,6}, Željko Ivezić^{2,6}, R. Lynne Jones^{2,6}, Mario Juric^{2,6}, David L. Kaplan⁸, Mansi M. Kasliwal¹, Michael S. P. Kelley⁴, Thomas Kupfer^{1,15,16}, Chien-De Lee¹¹, Hsing Wen Lin (林省文)^{11,17}, Ragnhild Lunnan³, Ashish A. Mahabal^{1,18}, Adam A. Miller^{19,20}, Chow-Choong Ngeow¹¹, Peter Nugent^{21,22}, Eran O. Ofek²³, Thomas A. Prince¹, Ludwig Rauch¹⁴, Jan van Roestel²⁴, Steve Schulze²³, Leo P. Singer^{9,10}, Jesper Sollerman³, Francesco Taddia³, Lin Yan¹, Quan-Zhi Ye (葉泉志)^{1,25}, Po-Chieh Yu (俞伯傑)¹¹, Tom Barlow¹, James Bauer⁴, Ron Beck²⁵, Justin Belicki²⁶, Rahul Biswas¹³, Valery Brinnel²⁷, Tim Brooke²⁵, Brian Bue²⁸, Mattia Bulla¹³, Rick Burruss²⁶, Andrew Connolly², John Cromer²⁶, Virginia Cunningham⁴, Richard Dekany²⁶, Alex Delacroix²⁶, Vandana Desai²⁵, Dmitry A. Dhev¹, Michael Feeney²⁶, David Flynn²⁵, Sara Frederick⁴, Avishay Gal-Yam²⁹, Matteo Giomi³⁰, Steven Groom²⁵, Eugene Hacquins²⁵, David Hale²⁶, George Helou²⁵, John Henning²⁶, David Hover²⁶, Lynne A. Hillenbrand³¹, Justin Howell²⁵, Tiara Hung⁴, David Imel²⁵, Wing-Huen Ip (葉永垣)^{11,32}, Edward Jackson²⁵, Shai Kaspi³³, Stephen Kaye²⁶, Marek Kowalski^{14,27}, Emily Kramer²⁸, Michael Kuhn¹, Walter Landry²⁵, Russ R. Laher²⁵, Peter Mao²⁶, Frank J. Masci²⁵, Serge Monkwewitz²⁵, Patrick Murphy³⁴, Jakob Nordin³⁰, Maria T. Patterson², Bryan Penprase³⁵, Michael Porter²⁶, Umaa Rebbapragada²⁸, Dan Reiley²⁶, Reed Riddle²⁶, Mickael Rigault³⁶, Hector Rodriguez²⁶, Ben Rusholme²⁵, Jakob van Santen¹⁴, David L. Shupe²⁵, Roger M. Smith²⁶, Maayane T. Soumagnac²⁹, Robert Stein¹⁴, Jason Surace²⁵, Paula Szkody⁶, Scott Terek²⁵, Angela Van Sistine⁸, Sjoert van Velzen⁴, W. Thomas Vestrand³⁷, Richard Walters²⁶, Charlotte Ward⁴, Chaoran Zhang⁸, and Jeffrey Zolkower²⁶

¹ Division of Physics, Mathematics and Astronomy, California Institute of Technology, Pasadena, CA 91125, USA; mjg@caltech.edu

² DIRAC Institute, Department of Astronomy, University of Washington, 3910 15th Avenue NE, Seattle, WA 98195, USA

³ The Oskar Klein Centre & Department of Astronomy, Stockholm University, AlbaNova, SE-106 91 Stockholm, Sweden

⁴ Department of Astronomy, University of Maryland, College Park, MD 20742, USA

⁵ Department of Physics, Auburn University, Auburn, AL 36849, USA

⁶ Department of Astronomy, University of Washington, Seattle, WA 98195, USA

⁷ B612 Asteroid Institute, 20 Sunnyside Avenue, Suite 427, Mill Valley, CA 94941, USA

⁸ Center for Gravitation, Cosmology and Astrophysics, Department of Physics, University of Wisconsin–Milwaukee, P.O. Box 413, Milwaukee, WI 53201, USA

⁹ Astrophysics Science Division, NASA Goddard Space Flight Center, MC 661, Greenbelt, MD 20771, USA

¹⁰ Joint Space-Science Institute, University of Maryland, College Park, MD 20742, USA

¹¹ Institute of Astronomy, National Central University, 32001, Taiwan

¹² The eScience Institute, University of Washington, Seattle, WA 98195, USA

¹³ The Oskar Klein Centre, Department of Physics, Stockholm University, AlbaNova, SE-106 91 Stockholm, Sweden

¹⁴ Deutsches Elektronensynchrotron, Platanenallee 6, D-15738, Zeuthen, Germany

¹⁵ Kavli Institute for Theoretical Physics, University of California, Santa Barbara, CA 93106, USA

¹⁶ Department of Physics, University of California, Santa Barbara, CA 93106, USA

¹⁷ Department of Physics, University of Michigan, Ann Arbor, MI 48109, USA

¹⁸ Center for Data Driven Discovery, California Institute of Technology, Pasadena, CA 91125, USA

¹⁹ Center for Interdisciplinary Exploration and Research in Astrophysics and Department of Physics and Astronomy, Northwestern University, 2145 Sheridan Road, Evanston, IL 60208, USA

²⁰ The Adler Planetarium, Chicago, IL 60605, USA

²¹ Computational Science Department, Lawrence Berkeley National Laboratory, 1 Cyclotron Road, MS 50B-4206, Berkeley, CA 94720, USA

²² Department of Astronomy, University of California, Berkeley, CA 94720-3411, USA

²³ Department of Particle Physics and Astrophysics, Weizmann Institute of Science, Rehovot 76100, Israel

²⁴ Department of Astrophysics/IMAPP, Radboud University Nijmegen, P.O.Box 9010, 6500 GL, Nijmegen, The Netherlands

²⁵ Infrared Processing and Analysis Center, California Institute of Technology, MS 100-22, Pasadena, CA 91125, USA

²⁶ Caltech Optical Observatories, California Institute of Technology, Pasadena, CA 91125, USA

²⁷ Institute of Physics, Humboldt-Universität zu Berlin, Newtonstraße 15, 124 89 Berlin, Germany

²⁸ Jet Propulsion Laboratory, Pasadena, CA 91109, USA

²⁹ Department of Particle Physics and Astrophysics, Weizmann Institute of Science 234 Herzl Street, Rehovot, 76100, Israel

³⁰ Institute of Physics, Humboldt-Universität zu Berlin, Newtonstraße 15, 12489 Berlin, Germany

³¹ Division of Physics, Mathematics, and Astronomy, California Institute of Technology, Pasadena, CA 91125, USA

³² Space Science Institute, Macau University of Science and Technology, Macau

³³ School of Physics & Astronomy and Wise Observatory, The Raymond and Beverly Sackler Faculty of Exact Sciences, Tel-Aviv University, Tel-Aviv 6997801, Israel

³⁴ Formerly of Caltech Optical Observatories, California Institute of Technology, Pasadena, CA 91125, USA

³⁵ Soka University of America, Aliso Viejo, CA 92656, USA

³⁶ Universit Clermont Auvergne, CNRS/IN2P3, Laboratoire de Physique de Clermont, F-63000 Clermont-Ferrand, France³⁷ Los Alamos National Laboratory, P.O. Box 1663, Los Alamos, NM 87454, USA

Received 2018 September 6; accepted 2019 January 21; published 2019 May 22

Abstract

The Zwicky Transient Facility (ZTF), a public–private enterprise, is a new time-domain survey employing a dedicated camera on the Palomar 48-inch Schmidt telescope with a 47 deg^2 field of view and an 8 second readout time. It is well positioned in the development of time-domain astronomy, offering operations at 10% of the scale and style of the Large Synoptic Survey Telescope (LSST) with a single 1-m class survey telescope. The public surveys will cover the observable northern sky every three nights in g and r filters and the visible Galactic plane every night in g and r . Alerts generated by these surveys are sent in real time to brokers. A consortium of universities that provided funding (“partnership”) are undertaking several boutique surveys. The combination of these surveys producing one million alerts per night allows for exploration of transient and variable astrophysical phenomena brighter than $r \sim 20.5$ on timescales of minutes to years. We describe the primary science objectives driving ZTF, including the physics of supernovae and relativistic explosions, multi-messenger astrophysics, supernova cosmology, active galactic nuclei, and tidal disruption events, stellar variability, and solar system objects.

Key words: (stars:) supernovae: general – surveys – (galaxies:) quasars: general

Online material: color figures

1. Introduction

The past decade has seen an explosion in time-domain astronomy driven by the availability of new instruments and facilities dedicated to repeated observations of large areas of sky. A number of surveys, e.g., Catalina Real-Time Survey (CRTS; Drake et al. 2009), Palomar Transient Factory (PTF/iPTF; Law et al. 2009), Panoramic Survey Telescope, and Rapid Response System (Pan-STARRS or PS; Kaiser 2004), All Sky Automated Survey for SuperNovae (ASAS-SN; Shappee et al. 2014), and the Asteroid Terrestrial-impact Last Alert System (ATLAS; Tonry et al. 2018) have opened up the exploration of temporal behavior from solar system objects to variable stars in the Galaxy to relativistic explosions across the universe. They have each employed differing modes of operation, e.g., the number of repeat visits to the same region of sky per night, inter-nightly cadence, choice of filters, etc., in addition to the varying capabilities of camera, telescope, and site to probe the potential discovery space.

The Zwicky Transient Facility (ZTF) consists of a wide-field imager on the Palomar 48-inch Oschin (Schmidt) telescope and an integral field unit spectrograph (IFUS) on the Palomar 60-inch

telescope optimized for spectral classification of relatively bright ($<19 \text{ mag}$) explosive transients. The former likely represents the height of what can be achieved with a single 1-meter class survey telescope. The resulting transients and variables will be bright enough that follow-up can be undertaken for well-defined samples by the existing suite of larger telescopes.

ZTF operates in a rich landscape of optical time-domain surveys. ASAS-SN is a long-term project dedicated to surveying the entire night sky. It consists of telescopes in both hemispheres and at a number of longitudes, and is well positioned to survey the entire night sky to about 18.5 mag each night. PS-1 has already delivered the definitive photometric catalog and deep reference imaging for the northern sky. PS-1 is now largely dedicated to the study of Near-Earth asteroids (NEOs). ATLAS visits a significant portion of the night sky every two nights, to about 19.5 mag. Although ATLAS is also tuned for investigating near-earth asteroids, it is reporting transients and publishing light curves for variable stars.

ZTF is undertaking a number of of different surveys (with cadence ranging from minutes to days). Its primary strength is its combination of depth and areal survey speed (Bellm 2016), which enable it to identify transients at earlier times relative to ASAS-SN and ATLAS, while covering a large fraction of the accessible night sky. Its productivity in the discovery of transients is enhanced by the availability of dedicated spectroscopic followup to provide routine classification. The IFUS on the robotic 60-inch telescope can undertake, without human intervention, nearly a dozen spectral classification observations per night. Finally, ZTF has been designed to be a stepping stone for LSST for transient (and variable) object astronomy. In

³⁸ B612 Asteroid Institute and DIRAC Institute Postdoctoral Fellow.³⁹ Hubble Fellow.⁴⁰ Moore-Sloan, WRF, and DIRAC Fellow.

Original content from this work may be used under the terms of the [Creative Commons Attribution 3.0 licence](https://creativecommons.org/licenses/by/3.0/). Any further distribution of this work must maintain attribution to the author(s) and the title of the work, journal citation and DOI.

particular, real-time alerts⁴¹ are being issued to brokers to enable community use of the data and to develop infrastructure for the LSST era. Although the main focus of ZTF (given its name) may initially appear to be transient science, it will also contribute to our knowledge and understanding of optical phenomena in both real-time and archival behaviors.

In this paper, we describe the science objectives that motivated the ZTF project. These are defined around particular areas of interest and we present here the expected outcomes and science deliverables of each: the physics of supernovae (SNe) and relativistic explosions (Section 3); multi-messenger astrophysics (Section 4); cosmological distances from Type Ia SNe (Section 5); cosmology with gravitationally lensed SNe (Section 6); active galactic nuclei (AGNs) and tidal disruption events (TDEs) (Section 7), Galactic science (Section 8), small solar system bodies (Section 9), and astroinformatics and astrostatistics (Section 10).

The following papers discuss performance and subsystems in detail. Bellm et al. (2019a) give a general overview of the ZTF system. C. Dekany et al. (2019, in preparation) provide an in-depth description of the design of the observing system. Bellm et al. (2019b) discuss the ZTF surveys and scheduler. Masci et al. (2019) detail the ZTF data system. Patterson et al. (2019) present the alert distribution system employed by ZTF. Mahabal et al. (2019) discuss several applications of machine learning used by ZTF. Tachibana & Miller (2018) present a new star/galaxy classifier developed for ZTF from the Pan-STARRS DR1 catalog (Chambers et al. 2016; Flewelling et al. 2016). Kasliwal et al. (2019) describe a web-based interface used by the ZTF collaboration to identify, track, and follow-up transients of interest.

2. The Zwicky Transient Facility

ZTF employs a new 576 megapixel camera (Dekany et al. 2016) with a 47 deg² field of view on the Samuel Oschin 48" Schmidt telescope (P48) at Palomar Observatory. It can observe 3760 deg² per hour to a 5 σ detection limit of 20.5 mag in r (with a 30 s exposure). The data-processing pipelines are managed by IPAC (Masci et al. 2019) with different branches for single-epoch images and catalogs, image subtraction, and moving objects. Alerts from difference images generated using the ZOGY algorithm (Zackay et al. 2016) are produced within 20 minutes of the raw image being taken with the ZTF instrument and distributed using the Kafka system (Patterson et al. 2019) operated by the University of Washington. These data packets contain thumbnails of the

discovery, reference, and difference images as well as a 30-day light-curve history for an alert.

Due to its funding profile, ZTF operates a unique observing strategy: 40% of the time is for public surveys, 40% for partnership observations, and the remaining 20% for Caltech programs. For the public surveys (Bellm et al. 2019b), the entire visible sky from Palomar is observed in g and r every three nights and the visible Galactic plane ($|b| < 7^\circ$) covered in g and r every night. Alerts from the public survey data are issued in real time. However, images and catalogs remain embargoed to all parties until public data releases (the first is scheduled for spring 2019 and every semester thereafter).

ZTF is issuing of order one million alerts per night. Note that other next generation surveys can also produce alerts at this scale, but they do not currently make them public. The 3-year duration of the project also means that about one billion sources will be observed about one thousand times. The final table of all individual source detections will thus be a trillion row catalog. ZTF can be regarded to be a precursor to LSST, operating at roughly the 10% scale (see Table 1 for further comparisons between ZTF, LSST, and other surveys).

A major motivation of ZTF was the detection and study of infant explosions. To this end, ZTF also has a dedicated follow-up capability in the form of the Spectral Energy Distribution Machine (SEDM) on the Palomar 60" telescope (Blagorodnova et al. 2018). This combines a low-resolution ($R \sim 100$) integral field unit (IFU) spectrograph with a multiband ($ugri$) photometer, and is optimized for classification and high observing efficiency. Sources detected by ZTF can be (automatically) submitted to the SEDM observing queue for swift observation. Below, we discuss each of the main science areas that ZTF is expected to explore. As with other surveys in the past, we also anticipate that the wealth of new data provided by ZTF will enable serendipitous discoveries of new classes of rare events (e.g., AT2018cow/ATLAS18qqn).

3. Physics of Supernovae and Relativistic Explosions

Supernovae will be the major class of non-moving transients detected by ZTF, and the expected rates across the range of different types of supernova support a number of systematic studies into these phenomena.

3.1. The Quest and Study of Infant Supernova Explosions

One of the boutique surveys carried out by ZTF is high-cadence (six times per night) observations of two thousand square degrees of the sky. This survey with good depth (20.5 mag) and good cadence was designed explicitly to find young SNe and undertake rapid follow-up studies. For massive star explosions, very early photometry from the ground and from space, available only for a handful of serendipitously observed events so far (e.g., Campana et al. 2006; Soderberg et al. 2008;

⁴¹ We use the LSST definition of an alert: a 5 σ change in R.A., decl., or flux, with respect to the reference sky. The resulting alert stream provides a comprehensive, real-time inventory of everything ZTF knows about the changing night sky, including not just transients, but also variable stars and solar system objects.

Table 1
A Comparison between ZTF, LSST, and Other Next-generation Surveys in Terms of Scale

Category	ATLAS	ASAS-SN	Pan-STARRS	ZTF	LSST
Number of total sources	...	1×10^8	1×10^{10}	1×10^9	37×10^9
Number of total detections	1×10^{12}	1×10^{11}	1×10^{11}	1×10^{12}	37×10^{12}
Annual visits per source	1000 ^c	180 ^d	60 ^c	300 ^a	100 ^b
Number of pixels	1×10^8	4×10^6 ($\times 4$)	1×10^9	6×10^8	3.2×10^9
CCD surface area (cm ²)	90	9	1415	1320	3200
Field of view (deg ²)	30	4.5	7	47	9
Hourly survey rate (deg ²)	3000	960	...	3760	1000
5 σ detection limit in r	19.3	17.3	21.5	20.5	24.7
Nightly alert rate	1×10^6	1×10^7
Nightly data rate (TB)	0.15	1.4	15
Telescope (m)	0.5	4×0.14	1.8	1.2	6.5
No. of telescopes	2 (6)	5	2	1	1

Notes.

^a - in 3 filters.

^b - in 6 filters.

^c - in 2 filters.

^d - in 2 filters.

^e - in 5 filters.

Gezari et al. 2008; Garnavich et al. 2016; Bersten et al. 2018) probes the early physics of explosion shock breakout and cooling (see Waxman & Katz 2017 for a recent review). For massive star explosions, early photometry (especially if it includes space UV data, e.g., Ofek et al. 2010; Gezari et al. 2008; Yaron et al. 2017; Ganot et al. 2016; Rubin & Gal-Yam 2017) provides powerful constraints on the nature of the progenitor and the parameters of explosion (e.g., its energy per unit mass, Rubin et al. 2016).

For Type Ia SNe, early photometry, especially in the UV, is a powerful probe for the existence of a possible mass-donor companion to the exploding white dwarf (Kasen 2010). Initial reports about a handful of events (e.g., Cao et al. 2015; Hosseinzadeh et al. 2017) motivate further exploration of this approach. Together, early photometric studies of both core-collapse and Type Ia SNe motivate a strong synergistic program combining ZTF data with rapid response *Swift* UV observations.

Discovery of SNe within 24 hr of explosion, enabled by the ZTF discovery, coupled with the ability to rapidly trigger the SEDM and other follow-up resources, would allow target-of-opportunity (ToO) spectroscopy of young SNe within hours of explosion. As shown by initial results using this “flash spectroscopy” technique on iPTF triggers (e.g., Gal-Yam et al. 2014; Khazov et al. 2016; Yaron et al. 2017), analysis of such early spectra of massive star explosions allows us to extract unique information about the distribution of circumstellar material (CSM) around exploding stars. The composition of such material, measured from emission line intensities, provides a direct measurement of the surface composition of the supernova progenitor as it was prior to explosion, while the

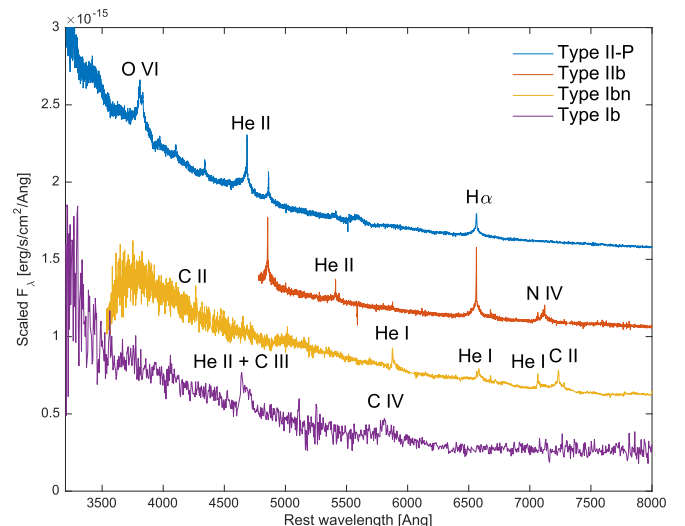


Figure 1. Collection of flash spectra from iPTF, showing the differing composition of the CSM around core-collapse SNe.

(A color version of this figure is available in the online journal.)

spatial distribution of the CSM, revealed by the transient nature of the emission lines, provides a record of the stellar mass loss just prior to explosion, with potentially critical clues about the SN explosion mechanism (Gal-Yam et al. 2014; Yaron et al. 2017). Temporal evolution of the emission lines within a night (Yaron et al. 2017) provides a measurement of the temporal evolution of the temperature in the emitting material, a valuable constraint on shock and interaction physics. Mapping the properties of flash-spectroscopy-revealed CSM across the range of SN types (Figure 1) is a key goal of ZTF.

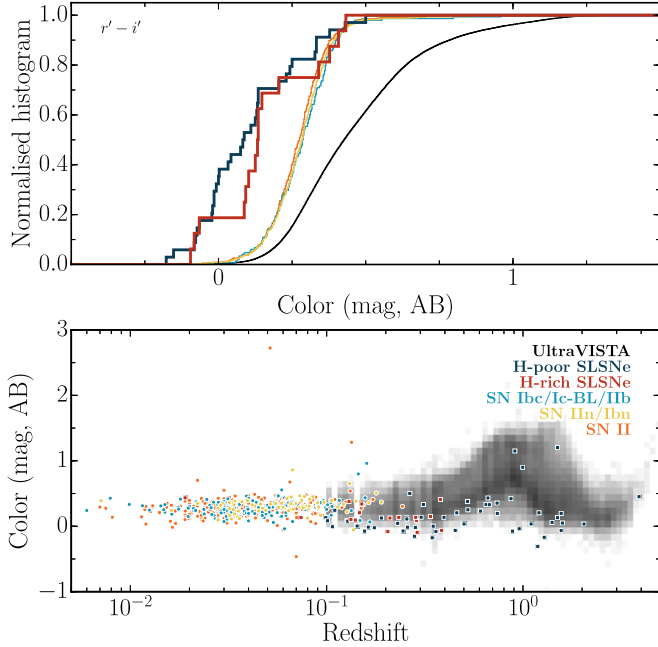


Figure 2. $r' - i'$ color distribution of 500 PTF/iPTF core-collapse SN host galaxies, SLSN host galaxies, and galaxies from the UltraVISTA survey. The top panel shows the cumulative distribution for all samples at $z < 0.7$. SLSN hosts are found in a part of the parameter space that is sparsely populated by galaxies, in general. The average host of an H-poor/-rich SLSN is 0.2/0.15 mag bluer than that of a regular core-collapse SN. Hence, host-galaxy properties could be used to identify infant SLSNe in the ZTF alert stream. Figure adapted from S. Schulze et al. 2019, in preparation. (A color version of this figure is available in the online journal.)

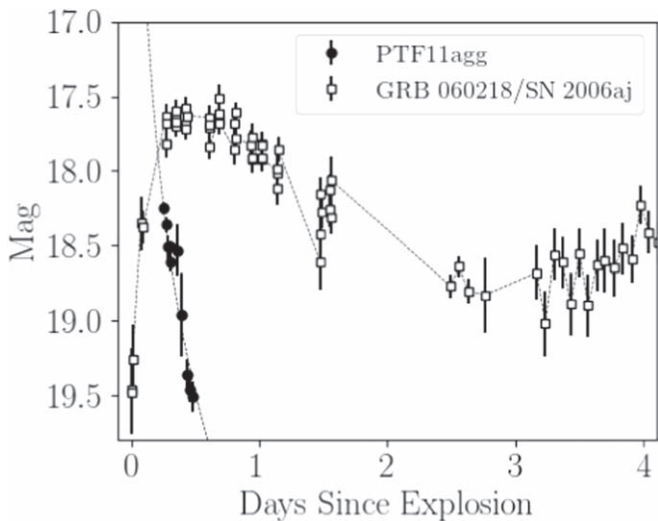


Figure 3. Light curves from the candidate on-axis dirty fireball PTF11agg and the low-luminosity GRB 060218/Ic-BL SN 2006aj. The rapid decay of PTF11agg is attributed to on-axis fading afterglow. The rise and fade of SN 2006aj at early times is likely due to shock cooling emission of SN ejecta.

3.2. New Insights into Interacting Supernovae

Type IIn supernovae are SNe, whose spectra show bright and narrow ($\lesssim 2000 \text{ km s}^{-1}$) Balmer emission lines (Schlegel & Petre 2006; Filippenko 1997; Gal-Yam 2017). Rather than a signature of the explosion itself, this spectral specificity is presumably the result of the interaction between the fast ejecta and a low-velocity, dense, hydrogen-rich, circumstellar medium that surrounded the star before it exploded. During the last decade, the physical picture governing SN IIn explosions and the wider family of “interacting” SNe—SNe whose radiation can be partially or completely accounted for by the ejecta crashing into a dense surrounding medium—has aroused a lot of interest.,

SNe IIn are presumably powered (at least partially) by the conversion of the ejecta kinetic energy into luminosity. This is a broad family of objects, with a wide variety of CSM masses ranging from $\gtrsim 10 M_{\odot}$ (e.g., Ofek et al. 2014a) to $0.01\text{--}0.1 M_{\odot} \text{ y}^{-1}$ (e.g., Kiewe et al. 2012). Such low-mass CSM events evolved faster, and are less luminous compared with high-mass CSM events (Ofek et al. 2014a). At the low-CSM mass, the IIn class is likely related to the flash spectroscopy SN events which have estimated CSM masses of the order of $\sim 10^{-3} M_{\odot}$ (e.g., Gal-Yam et al. 2014; Yaron et al. 2017), which are confined to the close vicinity of the progenitor star. ZTF will provide a unique insight into these objects. Type IIn Balmer narrow lines may persist for days (“flash spectroscopy”, Gal-Yam et al. 2014; Khazov et al. 2016; Yaron et al. 2017, weeks (e.g., SN 1998S, Li et al. 1998; Fassia et al. 2000, 2001; SN 2005gl, Gal-Yam et al. 2007; SN 2010mc Ofek et al. 2013b; PTF 12glz Soumagnac et al. 2019), or years (e.g., SN 1988Z, Danziger & Kjaer 1991; Stathakis & Sadler 1991; Turatto et al. 1993; van Dyk et al. 1993; Chugai & Danziger 1994; Fabian & Terlevich 1996; Aretxaga et al. 1999; Williams et al. 2002; Schlegel & Petre 2006; Smith et al. 2017; SN 2010jl Patat et al. 2011; Stoll et al. 2011; Gall et al. 2014; Ofek et al. 2014a). With its cadence and continuous coverage, ZTF will allow the study of the early and late photometric and spectral properties of interacting SNe and reveal the complete spectral evolution of these events. This will allow the investigation of the various physical scenarios leading to the presence of interaction signatures in the spectrum of SNe. ZTF has the potential to identify and follow-up hundreds of Type IIn SN. This will further lead to characterization of their CSM masses (e.g., Kiewe et al. 2012 Ofek et al. 2014b); probing their ejecta shock velocities; which is a probe of the internal explosion mechanism (e.g., Ofek et al. 2014b); and CSM geometry via the spectral and light-curve evolution (e.g., Soumagnac et al. 2019).

Furthermore, ZTF will give new insights into the precursors of SNe IIn. In recent years, it has become clear that a large fraction of SN progenitors show outbursts accompanied by large mass ejections (e.g., $\gtrsim 10^{-3} M_{\odot}$) months to years prior to

the terminal explosion of the star as a SN. In some cases, there are direct observations of such prior luminous outbursts (e.g., Foley et al. 2007; Pastorello et al. 2007; Mauerhan et al. 2012; Prieto et al. 2013; Corsi et al. 2014; Fraser et al. 2013; Ofek et al. 2013b, 2013a, 2014a, 2016; Strotjohann et al. 2015; Nyholm et al. 2017), and in other cases we detect high excitation emission lines, presumably due to the presence of massive circumstellar material around the SN progenitor (e.g., Gal-Yam et al. 2014; Khazov et al. 2016; Yaron et al. 2017). These observations suggest that the final evolution of massive stars is not well understood, as such eruptions do not occur in standard stellar evolution codes. This may be important for a better understanding of the SN explosion mechanism as these final stages determine the initial conditions to explosion simulations (e.g., Arnett & Meakin 2011; Quataert & Shiode 2012; Shiode & Quataert 2014; Fuller 2017; Fuller & Ro 2018). ZTF will cover the locations of multiple SNe IIn multiple times prior to the actual explosions, and will thus allow us to better study the precursors of SNe IIn. The public survey, with its all-sky footprint and uniform cadence (g and r band every three nights) will be particularly well suited to perform such study.

3.3. Superluminous Supernovae

Superluminous supernovae (SLSNe) are a rare class of transients with peak luminosities 10–100 times higher than ordinary core-collapse and Type Ia SNe, and total radiated energies in excess of 10^{51} erg (see e.g., Gal-Yam 2012 for a review). Their enormous energies cannot be explained by standard supernova models, and their progenitors and energy sources are still debated. Suggestions include either a central energy source (such as magnetar spin-down; Kasen & Bildsten 2010; Woosley 2010), strong interaction with dense CSM converting kinetic energy to radiation (Woosley et al. 2007; Chevalier & Irwin 2011; Sorokina et al. 2016), or the pair-instability explosion of a very massive star (Barkat et al. 1967; Gal-Yam et al. 2009).

ZTF will make progress in SLSN science in multiple ways. First, while more than 100 SLSNe from many different surveys have been reported to date (e.g., De Cia et al. 2018 (PTF), Lunnan et al. 2018 (PS-1)), fundamental population properties such as the SLSN rate are still only poorly constrained (Quimby et al. 2013; McCrum et al. 2015; Prajs et al. 2017). ZTF’s combination of sky coverage and cadence is ideal for selecting a large sample of SLSNe in a systematic fashion, thus determining population properties. More generally, increasing the sample of SLSNe with well-determined explosion dates and rise times, as well as color information also on the rise, is important for constraining the progenitors and energy sources of SLSNe, as the rise time encodes information about the diffusion timescale and hence the progenitor mass. For slowly declining SLSNe, the rise time is the main discriminator

between pair-instability and central-engine models (e.g., Nicholl et al. 2013; Lunnan et al. 2016).

Finally, ZTF’s capability to study young SNe (Section 3.1) extends to studying the early phases of SLSNe. Some SLSNe show a precursor “bump” on the rise, with typical timescales of ~ 10 days (Leloudas et al. 2012; Nicholl et al. 2015; Smith et al. 2016). It has been suggested that this feature is ubiquitous (Nicholl & Smartt 2016), but the presence of such a bump is poorly constrained due to a lack of well-sampled, early-time data in the majority of SLSNe. Understanding the physical nature of this precursor emission, and more generally what it implies for the explosion mechanism and extended structure of the progenitor star, holds great promise in shedding light on these enigmatic explosions.

While the light curve of the precursor can be recovered from ZTF data, securing spectra of the precursor requires detecting SLSNe before their light curve rises for several tens of days and before their luminosity exceeds -21 mag. SLSN host galaxies could be very useful in identifying infant SLSNe. SLSNe are preferentially found in star-forming dwarf galaxies with stellar masses of $< 10^{10} M_{\odot}$ and metallicities of < 0.4 solar metallicity (Lunnan et al. 2014; Leloudas et al. 2015; Perley et al. 2016; Schulze et al. 2018), whereas ordinary core-collapse SNe are found in more evolved galaxies (e.g., Kelly & Kirshner 2012). To illustrate this better, we display in Figure 2(a) subsample of 500 core-collapse SN host galaxies from PTF and iPTF surveys with detected hosts in r' and i' band (for details, see S. Schulze et al. 2019, in preparation), 53 H-poor and 16 H-rich SLSNe from Schulze et al. (2018) and galaxies from the UltraVISTA survey (McCracken et al. 2012). SLSNe are found in a part of the parameter space that is sparsely populated by galaxies in general. Moreover, the average host of H-poor/-rich SLSNe is 0.2/0.15 mag bluer than that of a regular core-collapse supernova (at lower redshift). Hence, host galaxy properties could be a valuable diagnostic to select infant SLSNe in real time.

3.4. Exploring the Diversity of Relativistic Explosions

In the final collapse and explosion of a massive star, $> 10^{51}$ erg of kinetic energy are liberated as the iron core collapses to a neutron star or a black hole, driving a spherical shock that unbinds the star (a supernova). A small subset ($\sim 0.1\%$) of these explosions exhibit even more extreme behavior: a relativistic bipolar jet is launched, drills through the envelope, and escapes to interstellar space. The jet produces a long-duration gamma-ray burst (GRB) lasting several seconds, and its collision with the circumstellar medium (CSM) produces an “afterglow” that radiates across the electromagnetic spectrum for days to months (Rees & Meszaros 1992).

To date, ~ 20 SNe have been spectroscopically confirmed in association with GRBs, beginning with the coincident discovery of GRB 980425 and SN 1998bw at $d = 40$ Mpc

(Galama et al. 1998; Kulkarni et al. 1998), All GRB-SNe have had envelopes stripped of hydrogen and helium (Type Ic) and high measured photospheric velocities ($\gtrsim 20,000 \text{ km s}^{-1}$). These “broad-lined” (BL) Ic SNe constitute $\sim 1\%$ of the local core-collapse rate, and their association with GRBs has led to the suggestion that GRBs and at least some Ic-BL SNe arise from a single explosion mechanism (Barnes et al. 2018; Sobacchi et al. 2017).

A major focus of scientific investigation over the past 20 years has been to understand the connections between these energetic Ic-BL supernovae with successful, observed jets and ordinary (non-relativistic) SNe without them. A minimum prerequisite for the launch of a jet is the formation of a “central engine” from the collapsing core: a highly magnetized neutron star or rapidly accreting black hole. However, even if such an engine forms, a number of other conditions must also be met for us to observe the jet as a GRB. First, the jet must be nearly baryon-free (else the available energy is insufficient to accelerate the ejecta to ultra-relativistic velocities), and gamma-ray emission will be stifled by pair production. Next, the jet must successfully escape the star without being smothered by the stellar envelope. Finally, the jet must be directed at Earth.

If any of these conditions are not met, a variety of different empirical phenomena are predicted:

- (a) A jet with too many baryons ($> 10^{-4} M_{\odot}$) is known as a dirty fireball. Given the energy budget of the explosion, it can attain only a moderate Lorentz factor ($\Gamma \sim 5\text{--}10$), so while it successfully escapes the star and should produce a luminous afterglow, it will not produce *significant* high-energy emission and thus not trigger gamma-ray instruments (Dermer et al. 1999).
- (b) A jet which fails to escape the stellar envelope is sometimes termed a choked jet or a failed jet (Mészáros & Waxman 2001). However, the jet energy may be transferred into a shock wave that propagates through the star and breaks out at the surface: this may produce a low-luminosity gamma-ray burst (LLGRB; Bromberg et al. 2011; Nakar 2015) and a Type Ic-BL SN.
- (c) In most cases, the viewing angle exceeds the jet half-opening angle. Such an off-axis jet (clean or dirty) that escapes the star will result in an orphan afterglow (Rhoads 1997). The relativistic beaming of such an event means that there will be suppressed (or a lack of) observed gamma-ray emission. The afterglow will brighten as the shock slows and the relativistic beaming cone widens to include Earth (e.g., van Eerten et al. 2010).

A census of these phenomena is required to quantify key physical processes in core-collapse SNe and their connection to relativistic transients. How many SNe actually produce central engines? Why do “classical” GRB jets accelerate only a tiny

fraction of their mass: is the fractional mass fundamental to the phenomenon, or the tip of the iceberg of a wider range of jet phenomena? In particular, do LLGRBs result from jets getting choked within the star? And, finally, how accurate is our understanding of beaming in GRBs?

We are addressing this area via three surveys. The partnership moderate-cadence survey (Section 3.1) is well suited to find rapidly fading afterglows. In fact, the moderate-cadence survey was based on the success of a pilot project undertaken with PTF (which resulted in a cosmological afterglow candidate, PTF11agg; see Figure 3, Cenko et al. 2013). A nightly cadence survey, another boutique survey, is squarely aimed at LLGRB and LLGRB-like SNe such as SN 2006aj (Soderberg et al. 2006) and iPTF 16asu (Whitesides et al. 2017), as well as orphan afterglows. We have undertaken archival analysis of iPTF data and devised excellent filters to reject false positives for these two surveys (M dwarfs and dwarf novae; Ho et al. 2018). Finally, the public all-sky three-night survey will result in SEDM classifications of 500 SNe per semester, of which a few percent will be Ic/BL SNe.

3.5. Rare Transients in the Local Universe

The luminosity gap between novae and supernovae has recently been populated with a variety of faint and fast-evolving transients in the local universe (Kasliwal 2012). PTF/iPTF, with its untargeted wide-field search and committed spectral classifications with the Palomar 200-inch and SEDM (peaking at 700 classifications per year) resulted in several interesting transients including rapidly evolving Type Ic SNe like SN 2010X and iPTF 14gqr (Kasliwal et al. 2010; De et al. 2018; see also SN 2005ek), and significantly increased the samples size of calcium-rich gap transients (Perets et al. 2010; Kasliwal et al. 2012). However, the physical nature of these explosions remains largely debated as their faint and fast-evolving light curves (and hence low ejecta mass) point to very low-mass progenitors, unlike the population of Type Ia and core-collapse SNe. Suggested progenitor channels include tidal disruptions of low-mass white dwarfs by a neutron star or black hole (Sell et al. 2015), He shell detonations on the surface of white dwarfs (Bildsten et al. 2007), or core-collapse explosions of highly stripped massive stars (Kleiser & Kasen 2014; Tauris et al. 2013). Yet the small number of confirmed events leaves considerable uncertainty about the intrinsic properties of these intriguing transients.

ZTF, with its order of magnitude improvement in survey speed over PTF, will be a powerful tool to discover large samples of these faint and fast-evolving explosions in the local universe. This will aid not only in understanding the distribution of the intrinsic properties of this population (e.g., ejecta masses, explosion energies and peak luminosities), but also shed light on their progenitors via their host environments. For instance, the old and remote environments of the class of

Ca-rich gap transients (a total of eight confirmed events thus far) suggest their association with a very old progenitor population that has traveled far away from their host galaxies, consistent with progenitors arising from old white dwarf binary systems (Lunnan et al. 2017; see also De et al. 2018). On the other hand, the star-forming host galaxies of the fast Type Ic SNe like SN 2010X and SN 2005ek are consistent with white dwarf progenitors as well as core-collapse explosions of “ultra-stripped” massive stars (Moriya et al. 2017).

The number of false positives is significantly reduced by the requirement that candidates be in the apparent proximity of galaxies with $z < 0.05$. The resulting spectroscopic load (for classification) then becomes manageable with the resources available to the ZTF partnership (e.g., Palomar 200-inch, Nordic Optical Telescope, Liverpool Telescope, and peer-reviewed Gemini allocations). Early follow-up allows one to directly constrain the pre-explosion properties of the progenitor star. Such techniques have already been demonstrated to be a powerful probe of the nature of the progenitor in the case of Type Ia (Nugent et al. 2011) and core-collapse SNe (Yaron et al. 2017), and will be important for shedding light on the progenitors of these rare transients. Finally, ZTF will also be important in constraining the rates of these transients (which are otherwise poorly constrained due to the small number of events) that likely have important effects on the chemical evolution of the universe (Mulchaey et al. 2014). Current estimates of the rate of Ca-rich gap transients that include the survey efficiencies of PTF suggest that their rates are nearly half of the Type Ia supernova rate. This indicates that ZTF is expected to find more than 20 such events per year (Frohmaier et al. 2018). Rate constraints will also benefit from such events initially detected by ongoing time-domain surveys.

3.6. A Larger Sample of Stripped Envelope Supernovae and their Host Galaxies

The stripped envelope supernovae (SE SNe) samples currently available in the literature are mainly targeted (i.e., 34 SE SNe in Taddia et al. 2018b, CSP), non-homogenous (i.e., collections by Cano 2013; Lyman et al. 2016, and Prentice et al. 2016), or rather small (i.e., 20 SNe in Taddia et al. 2015, SDSS II). ZTF will allow us to build a large, homogeneous SE SN sample. Its untargeted nature will diminish the bias toward metal-rich SN host galaxies, as it will enable finding SE SNe also in low-luminosity and low-metallicity galaxies. With this sample, the main scientific questions are related to understanding the nature of the progenitor stars of SE SNe. By modeling the light curves of our SE SNe sample, we aim to determine the range of the SN explosion parameters. Besides the semi-analytic Arnett model (Arnett 1982), we can make use of more sophisticated hydrodynamical codes, such as HYDE (Ergon et al. 2015) and SNEC (Morozova et al. 2015), to estimate the explosion parameters. We know from the literature

that most SE SNe have relatively narrow light curves, suggesting moderate to low ejecta mass (order of 2–4 M_{\odot}). However, with iPTF we initiated a sample study of light curves, identifying a number of unusual SE SNe. For example, we discovered a dozen SE SNe with broad light curves that might have massive progenitors, e.g., iPTF15dtg (Taddia et al. 2016) and PTF11mnb (Taddia et al. 2018a), and/or alternative powering mechanisms (e.g., magnetar). We also studied iPTF 14gqr, an SN with a much narrower light curve than average, very likely arising from an ultra-stripped progenitor De et al. (2018). We expect to considerably increase the size of these samples with the forthcoming ZTF data. To increase the sample size is particularly important for these rare SNe, which we have hitherto followed only in a few cases. The stellar initial mass function is steep, and to sample the most massive progenitors simply requires a large number of events. With ZTF we will be able to discover these SNe routinely, and we aim to follow them up to classify them and to characterize their light curve shapes.

With iPTF we also discovered and investigated the unusual presence of early light curve excesses in some SNe Type Ic. This is compatible with the presence of an extended envelope (tens to hundreds of solar radii) around their progenitor stars (e.g., Taddia et al. 2016). With the higher cadence of ZTF, we aim to routinely study these early emission excesses, to get a better constraint on the progenitor radius of SE SNe. ZTF will also provide more early color information (g and r band from P48) of the SN emission. This will allow us to build bolometric light curves and temperature profiles at early epochs, which provide information on the degree of ^{56}Ni mixing in the SN ejecta. In summary, with ZTF we aim to observe a substantial sample of SE SNe with tight pre-explosion limits, pre-maximum coverage, and multiband light curves over a range of host galaxy properties.

3.7. Failed Supernova Shock Breakouts

Core collapse of a massive star may result in a “failed” SN, where the core promptly forms a black hole after the accretion shock fails to explode the star. While this fate has long been suggested for very-high-mass stars at low metallicity, there is mounting evidence that failed SNe may also occur in red supergiants (RSGs) with solar metallicity. First, there is a dearth of $>18 M_{\odot}$ RSG SN progenitors—the “missing RSG problem” (Kochanek et al. 2008; Smartt et al. 2009; Horiuchi et al. 2014; Smartt 2015). Also, a significant fraction of core-collapses resulting in failed SNe naturally explains the gap between the neutron star and black hole mass distributions (Kochanek 2014). The most dramatic evidence is the disappearance of a $10^{5.3} L_{\odot}$ RSG (Gerke et al. 2015; Adams et al. 2017) discovered by an ongoing survey monitoring a million RSGs in nearby galaxies with deep optical imaging (Kochanek et al. 2008).

Searching for disappearing core-collapse progenitors is observationally expensive and cannot feasibly be scaled up enough to tightly constrain the rates and progenitor properties. Moreover, with this approach candidates are only identified months (or years) after core collapse, making detailed observations of the event and its immediate aftermath impossible.

However, the disappearance of the progenitor is not the only possible signature of these events. Models predict that even if the energy released by the core collapse of a RSG fails to result in a SN, the loss of gravitational binding energy from the neutrino emission may result in a low-velocity ($\sim 100 \text{ km s}^{-1}$) ejection of the weakly bound hydrogen envelope (Nadezhin 1980; Lovegrove & Woosley 2013), giving rise to a faint ($\sim 10^6 L_{\odot}$) but long-lived (months to years) recombination-powered transient (Lovegrove & Woosley 2013; Fernández et al. 2018). Though the temporal sampling is coarse, the observations of the failed SN candidate reveal a several month long transient consistent with this prediction (Adams et al. 2017). Given the likely low rate of failed SNe, this type of transient is too faint to be discovered with supernova surveys, but with the ZTF the shock breakout associated with these events could be discovered for the first time, triggering spectroscopic follow-up and a search for the subsequent fainter recombination-powered transient.

Although the shock breakouts of normal SNe are very short (seconds to hours) and radiate primarily in the UV and X-rays, the shock breakout from the low-energy, neutrino-mediated shock of a failed SN is predicted to have a duration of a few days and be thermalized to a temperature of $\sim 10^4 \text{ K}$, with a luminosity of $\sim 10^7 L_{\odot}$ (Piro 2013; Lovegrove et al. 2017; Fernández et al. 2018).

Observations of both the shock breakout and the subsequent recombination phases would provide a unique confirmation that a failed SN has occurred. The shock breakout luminosity, temperature, and duration together with the luminosity and duration of the subsequent recombination-powered transient can constrain the progenitor radius, the explosion energy, and the ejected mass.

Though the expected ZTF discovery rate of failed SN shock breakouts is low, this approach represents the only feasible way to promptly discover and observe the birth of a new black hole from stellar core collapse for the very first time. The only false positives are novae (which, due to their luminosity function, are limited to galaxies no further than 10 Mpc). ZTF is well suited to this project given its depth.

3.8. Bright Transient Survey

Two science drivers motivated the Bright Transient Survey (BTS). First, one of the approaches for finding electromagnetic (EM) counterparts to neutron star mergers is to target galaxies in the localization constraints (including redshift) provided by

the gravitational wave (GW) facilities (e.g., Gehrels et al. 2016). However, the quantitative efficiency of this method requires the knowledge of the redshift completeness fraction (RCF) of these catalogs. We measure RCF using SNe as markers of galaxies (regardless of their luminosity). Preliminary estimates of the RCF find that $\sim 75\%$ of $z < 0.03$ galaxies are cataloged, based on observations of $m_{\text{peak}} < 17 \text{ mag}$ SNe from the ASAS-SN survey (Kulkarni et al. 2018). Next, there is widespread recognition of increased precision for Ia SN cosmology at low redshift, $z < 0.15$ (and discussed in great detail in Section 5). To satisfy these two projects a significant fraction of SEDM has been set aside to spectrally classify bright transients ($\lesssim 19 \text{ mag}$) with the expectation of completeness to 18.5 mag. Such bright transients will not only be found by the ZTF public survey but also by ASAS-SN, ATLAS and PS. We plan to publish a yearly catalog spelling in detail observational conditions so that the sample can be used to compute reliable rates. With the data in hand it appears that we are on course to classify 500 bright transients every semester.

4. Multi-messenger Astrophysics

Multi-messenger astrophysics is a growing methodology in astronomy and to this end we have built-in ToO capability. Multi-messenger astrophysics has three science objectives: (i) identifying electromagnetic (EM) counterparts to neutrino triggers from IceCube; (ii) identifying afterglows to short hard gamma-ray bursts from the *Fermi* satellite; and (iii) identifying electromagnetic counterparts to gravitational wave (GW) triggers from LIGO/Virgo.

4.1. Identifying Electromagnetic Counterparts to Neutrinos

The IceCube Neutrino Observatory has discovered a diffuse flux of high-energy neutrinos (Aartsen et al. 2015; IceCube Collaboration 2013). However, until recently, no compelling evidence for spatial or temporal clustering of events had been identified and the origin of the neutrinos was unknown (Aartsen et al. 2017a, 2015). The consistency of the spatial distribution with an isotropic flux points to a predominantly extragalactic origin for the neutrinos. Multi-messenger studies are key to identifying the neutrino sources, through detection of their EM counterparts. ZTF's all-sky coverage and high cadence will play a crucial role in detecting potential optical counterparts to astrophysical neutrinos, such as flaring blazars, choked-jet supernovae (Senno et al. 2016), CSM-interacting SNe (Murase et al. 2011; Zirakashvili & Ptuskin 2016), and tidal disruption events (Lunardini & Winter 2017). Our goal is to identify the neutrino sources through two complementary approaches.

First, a ToO program will select the most promising astrophysical neutrino candidates in real time (Aartsen et al. 2017b) from IceCube, and trigger rapid follow-up observations with ZTF to target fast-evolving transients (such as GRB

afterglows). ZTF’s ToO marshal will enable prompt collection of early photometry. These observations, in combination with upper limits provided by the regular all-sky survey, will allow tight constraints to be placed on the explosion time of GRBs or choked-jet SNe. Such temporal constraints are crucial to establish the causal connection between the neutrino and the potential optical counterpart. The effectiveness of ToO follow-up in identifying possible optical counterparts is already well established.

One interesting candidate, SN PS16cgx, was found during the Pan-STARRS optical follow-up of the first publicly released high-energy neutrino alert (Smartt 2016). With a tentative classification as a broad-lined Type Ic, the object could belong to the rare class of objects that is also associated with long GRBs, and hence a potential neutrino source.

Another follow-up of a more recent high-energy neutrino event revealed a spatially coincident blazar, TXS 0506+056, which was found by *Fermi*-LAT to be in flaring state (Aartsen et al. 2018). The coincidence triggered further multi-wavelength follow-up, leading to the discovery of very-high-energy gamma-ray emission by MAGIC. Study of archival optical data revealed a rise of ~ 0.5 mag in V-band over the preceding 50 days. Those findings are consistent with Fermi blazars contributing $< 10\%$ to the diffuse neutrino flux (Murase et al. 2018).

Second, while only a handful of the highest-energy neutrinos, with a $> 50\%$ chance to be of astrophysical origin (~ 10 per year), are suitable for the ToO program, there are many more detected neutrinos that could also have optical counterparts. We can utilize ZTF’s all-sky survey to access these lower-energy cosmic neutrinos, which are buried in a background of atmospheric neutrinos. With an all-sky, real-time search, in which we correlate all optical transients found by ZTF with all neutrino candidates detected by IceCube, we will target potential optical transient counterparts (e.g., SNe, TDEs) accounting for position, time, and neutrino energy. In particular, an online stream of approximately 100 neutrinos per day will be cross-matched with all detected ZTF transients during each night of observation. Positive correlations will trigger a dedicated follow-up campaign for potential optical transient counterparts that will also enable us to acquire a complete flux-limited catalog (to 20th mag) of classified sources as potential neutrino counterparts. IceCube’s most sensitive sky region (the Northern sky; Aartsen et al. 2017a) is excellently matched by ZTF’s coverage of the Northern sky.

The discovery of the origin of high-energy neutrinos would be a breakthrough for the emerging field of neutrino astronomy, and would furthermore reveal the much sought-after sources of high-energy cosmic rays. More specifically, the detection of neutrinos from choked-jet SNe would offer a direct window to the internal dynamics of those sources. It would constrain the composition, energetics, and Lorentz boost factor of relativistic outflows leaving the collapsing star, and resolve the currently

uncertain emission mechanism for GRBs. Deciphering the processes in the cores of collapsing stars hidden from electromagnetic observations is one of neutrino astronomy’s key science goals.

4.2. Identifying Afterglows to Short, Hard Gamma-Ray Bursts

The recent discovery of broadband electromagnetic radiation associated with gravitational waves from a binary neutron star merger (Abbott et al. 2017c) has ushered in a new era of multi-messenger astrophysics. One of the more unexpected results from this discovery was the detection of a low-luminosity short gamma-ray burst (GRB 170817A; Goldstein et al. 2017) just 1.7 s after the binary neutron star (BNS) merger. With $E_{\gamma, \text{iso}} \approx 3 \times 10^{46}$ erg (Abbott et al. 2017b), GRB 170817A is 3–4 orders of magnitude less energetic than all previous short GRBs with secure redshift measurements.

The explanation for this low-luminosity gamma-ray emission remains hotly debated. One possibility is that an ultra-relativistic jet was launched following the binary neutron star merger, but our viewing angle is slightly off-axis (though still within the envelope) of a “structured jet” (Abbott et al. 2017b). As a result, the gamma-ray luminosity we observe is significantly reduced, but some other observer in the universe would have seen a classical short GRB following the binary neutron star merger. Alternatively, the gamma-ray emission may have been powered by a (quasi)spherical, mildly relativistic outflow. Such emission may arise naturally from the “cocoon” formed when a jet fails to penetrate the neutron-rich material dynamically ejected prior to the merger (Kasliwal et al. 2017; Gottlieb et al. 2018).

Regardless of the origin, it is clear that the gamma-ray emission from a NS merger can be observed from outside the narrow opening angle of the ultra-relativistic jets of classical (i.e., high $E_{\gamma, \text{iso}}$) short GRBs. Thus, low-luminosity, short GRBs may offer a new means to identify the r-process kilonovae following neutron star mergers, independent of any gravitational-wave trigger.

No short-duration GRBs have been conclusively identified within 200 Mpc (the horizon distance for BNS mergers from Advanced LIGO at design sensitivity) to date, despite dozens of robust host associations from the well-localized *Swift* sample (e.g., Berger 2014). However the Gamma-Ray Burst Monitor (GBM; Meegan et al. 2009) on board the *Fermi* satellite triggers on $\approx 4\times$ more short-duration GRBs per year than *Swift* (with even more detected via ground-based pipelines; Briggs & Fermi GBM Team 2017). Few (if any) of these GBM short-duration GRBs are followed up with optical facilities (see, e.g., Golkhou et al. 2018), due primarily to their coarse localizations from several hundred up to ~ 1000 deg².

With the large field of view and automated transient identification pipeline of ZTF, we will follow a sample of

short-duration GRBs from the *Fermi*-GBM to search for kilonova counterparts. While most such GRBs will be at distances $\gg 100$ Mpc (the approximate distance out to which the GBM could detect GRB 170817A; Abbott et al. 2017b), within this volume the rate of BNS mergers is $\approx 6 \text{ yr}^{-1}$ (Abbott et al. 2017c). If all BNS mergers have a gamma-ray signal of comparable luminosity to GRB 170817A (as may be expected in cocoon models), ZTF will be capable of finding several counterparts per year, even before the next LIGO and Virgo observing run begins. For those more distant events, ZTF will be sensitive to the bright but rapidly fading afterglow emission, allowing robust host association and redshift and offset measurements.

4.3. Identifying Electromagnetic Counterparts to Gravitational Wave Transients

Pinpointing EM counterparts to neutron star mergers has the potential to unlock a wide range of new astrophysics, as illustrated by GW170817. For instance, detailed photometry and spectroscopy coupled with reliable rate estimates will quantify how prolific a site of r-process nucleosynthesis they are and whether they can explain the observed solar abundance of heavy elements (e.g., Drout et al. 2017; Kasliwal et al. 2017; Kasen et al. 2017; Hotokezaka et al. 2018). EM counterparts are crucial to reliable measurements of the Hubble constant (Schutz 1986; Abbott et al. 2017a), which is still a topic of interest (Riess et al. 2018a). Neutron star mergers are also unique laboratories to study jet physics (e.g., Lamb & Kobayashi 2018; Granot et al. 2017; Lazzati et al. 2018; Gill & Granot 2018; Nakar & Piran 2018), especially the wide-angle mildly relativistic cocoon breakout seen in GW170817 (Hallinan et al. 2017; Mooley et al. 2018; Dobie et al. 2018; Alexander et al. 2018; Troja et al. 2018).

With its combination of mapping speed and depth, ZTF is well poised to identify EM counterparts given its location at Palomar Observatory (facilitating prompt response), although we note that there are other facilities that may be more optimal for this purpose. Based on pessimistic models for optical emission Ghosh et al. (2017) worked to optimize the follow-up strategy, distributing observations to cover the gravitational-wave error region (which could be 1000 deg^2 , depending on the number of detectors involved; Singer et al. 2014) and showed that ZTF should be able to detect a significant fraction of sources in the upcoming third GW observing run. Given how bright the early-time emission was from GW170817 (e.g., Drout et al. 2017; Kasliwal et al. 2017; Arcavi et al. 2017; Nicholl et al. 2017), we may even be able to see a significant fraction with shorter observations, but we are baselining our plans to be able to detect counterparts $10\times$ fainter than GW170817 at 120 Mpc.

5. Cosmological Distances from Type Ia Supernovae

The use of Type Ia supernovae as distance indicators led to the discovery of the accelerating universe (Riess et al. 1998; Perlmutter et al. 1999), attributed to the existence of a new cosmic component dubbed “dark energy” (see Goobar & Leibundgut 2011 for a review). Perhaps the “simplest” explanation for dark energy is the one introduced already by Einstein, the cosmological constant, Λ . Whereas Λ would seem to correspond conceptually to the vacuum energy density expected from quantum field theory, the measured value of ρ_{DE} is at least 60 orders of magnitude too small, rendering the association extremely uncertain. Given the current lack of theoretical understanding, the quantity used to parameterize the nature of dark energy (DE) is the dimensionless equation of state parameter, built by the ratio of the pressure to energy density of the dark energy cosmological fluid, $w = p_{\text{DE}}/\rho_{\text{DE}}c^2$, which for the vacuum energy associated with Λ becomes $w = -1$. Using the most recent SN Ia compilations in Betoule et al. (2014) and Scolnic et al. (2018) in combination with CMB and BAO data, attempts have been made to explore alternative dark energy models. While Einstein’s Λ in a flat universe is favored by the current observations, several competing models based on well-founded physics remain unchallenged (Dhawan et al. 2017). It has long since been recognized that the low-redshift anchoring SN Ia sample is crucial to discern between dark-energy models (Goliath et al. 2001; Astier et al. 2014). Besides the limited statistics, the diverse origin, filter sets and lack of precise calibration makes the current low- z SN Ia sample the main contributor to the systematic uncertainties of the estimates of the dark energy equation of state (Scolnic et al. 2018; Foley et al. 2018). The ZTF public survey, in combination with a partnership i -band four-day cadence of 6700 deg^2 , is expected to yield nearly 2000 spectroscopically identified SNe Ia (Feindt et al. *in prep.*) over three years, with a subpercent absolute calibration with a redshift distribution shown in Figure 4 and median peak magnitudes of 18.26 mag and 18.32 mag in g - and r -band, respectively. The ZTF survey can provide a complete and unbiased SN Ia sample for $z < 0.1$.

With the ZTF plans of spectroscopic follow-up and management of the follow-up sample, this should be a multiband, well-sampled, spectroscopically confirmed, unbiased and close to complete data set, with well understood selection properties. The data set will be ideal for studying the supernova population, for example, exploring the effect of the local host environment on standardization of supernovae that have been found in other studies (see Roman et al. 2018, and references therein).

ZTF, along with other surveys discovering high rates of SNe Ia, such as ATLAS, Pan-STARRS and ASAS-SN, or the Foundation effort (Foley et al. 2018), aiming at building up multicolor light curves for many hundred SNe Ia, are providing

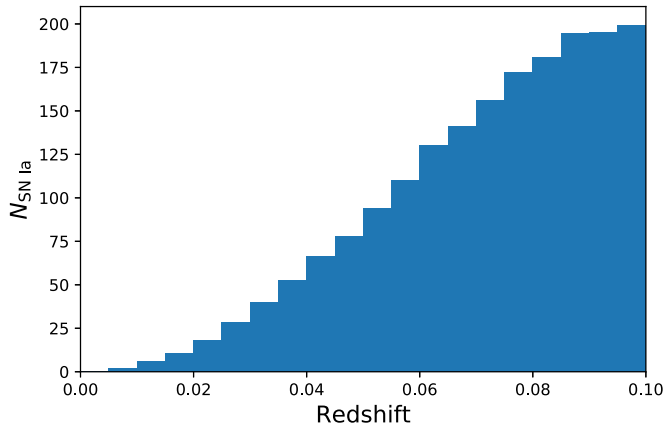


Figure 4. Redshift distribution of the 2000 expected SN Ia cosmology spectroscopic sample, where the upper redshift limit $z = 0.1$ is chosen to mitigate the impact from Malmquist bias. Only supernovae discovered >10 days prior to light-curve maximum are included.

(A color version of this figure is available in the online journal.)

the critical anchoring samples for cosmology. The ZTF survey offers specific advantages related to the understanding of systematic effects that need to be controlled to make major progress in precision cosmology with SNe Ia, e.g., corrections for selection effects like Malmquist bias. These require a knowledge of the underlying supernova population (rates, luminosity functions, and galaxy occupation distributions) conditioned on (possibly local; Rigault et al. 2018) host galaxy properties. The difficulties related to the sampling of SNe from different host galaxy populations at low- z compared with the high- z counterparts can be appreciated in Figure 2 in Jones et al. (2018), showing significant differences between the low and high-redshift host galaxy stellar mass. Thanks to the better depth than, e.g., ASAS-SN and ATLAS, the ZTF SN Ia lightcurves are sampled over longer time, both before and after peak, and thus better suited for detailed comparisons with high- z samples from LSST and WFIRST, a critical aspect of checks for possible demographic changes in the populations of SNe used for distance measurements. Furthermore, the extremely early SN detection, averaging at 13 days prior to light-curve maximum, can be used to study the evolution of color excess, and thereby constrain the location of dust clouds dimming the SN light, a crucial aspect in the understanding of the color corrections needed to standardize SNe Ia for cosmological distance estimations (Bulla et al. 2018a, 2018b). The ZTF SN Ia sample will also shed light into the impact of dimming by dust in the intergalactic medium (Goobar et al. 2018), an effect currently not included in the cosmological fits with SNe Ia. ZTF will thus provide an excellent anchoring sample with which to quantify the key systematic uncertainties that will limit future high- z surveys from LSST and WFIRST. Similarly, ZTF will provide an independent SN Ia sample to measure the Hubble constant, H_0 , where a nearly 4σ tension has been

claimed between the local measurements of the expansion rate based on SNe Ia calibrated with Cepheids (Riess et al. 2016, 2018b, 2018a) and the value derived from *Planck* measurements of the angle subtended by the sound horizon as observed in CMB temperature fluctuations (Planck Collaboration et al. 2016). Finally, thanks to the large effort on spectroscopic follow-up of both Type Ia and core-collapse supernovae, these data will serve as training samples for classification of future and ongoing surveys continuing to hold legacy value for future deeper surveys, even after the completion of ZTF.

The measured redshift of galaxies is given by the combined effects of cosmological expansion and the peculiar motion induced by the surrounding gravitational potential. The Type Ia supernovae detected by ZTF fall into a key distance range where the standardized luminosity can be used to determine the cosmological distance without significant dependence on cosmological parameters, while the volume of the universe is sufficient to produce large samples of supernovae every year. Such a large sample can then be used to constrain the correlations between the peculiar velocities in order to study the structure of the local universe. To first order, this can be done by measuring the large mode of correlation, a velocity dipole or bulk flow, which can test whether the nearby distribution of galaxies and clusters matches our expectation (e.g., Feindt et al. 2013). Additionally, the correlation across all scales can also be used to directly measure the local growth factor of structure more precisely than has been done before (e.g., Howlett et al. 2017b). This will directly test recent claims of deviations between the measured structure of the nearby universe and the Λ CDM predictions derived from the *Planck* CMB map (Hildebrandt et al. 2017; Köhlinger et al. 2017). The ZTF SN Ia peculiar velocity sample will populate the northern hemisphere in a way that current and future (e.g., TAIPAN and WALLABY, da Cunha et al. 2017) southern galaxy peculiar velocity samples do not. The much more precise distances derived from SNe mean that the few thousand ZTF SNe would provide similar statistical constraints as the many times larger galaxy samples (Koda et al. 2014; Howlett et al. 2017a). More importantly, the small SN Ia intrinsic dispersion fraction of distance estimate errors means that the potential for systematic uncertainties is much reduced (Barone-Nugent et al. 2013; Rigault et al. 2013; Nordin et al. 2018). A further key advantage of the ZTF SN peculiar velocity sample will be the small and well understood Malmquist bias.

6. Cosmology with Gravitationally Lensed Supernovae

One of the foundations of Einstein’s theory of general relativity is that matter curves the surrounding spacetime. For the rare cases of nearly perfect alignment between an astronomical source, an intervening massive object, and the

observer, multiple images of a single source can be seen by the observer, a phenomenon known as strong gravitational lensing. Gravitationally lensed supernovae (gLSNe), and in particular lensed SNe Ia, have the potential to directly constrain the expansion rate of the universe through the time delay between images (Refsdal 1964) due to their well-known light curve shapes. Time-delay measurements can also provide powerful leverage for the studies of dark energy in complementary ways to those from standard supernova cosmology, BAO, CMB and weak lensing (Linder 2011). Although many strongly lensed galaxies and quasars have been detected to date, finding this special configuration for supernovae has proved extremely difficult: only two multiple-imaged supernovae have been discovered to date (Goobar et al. 2017; Kelly et al. 2016).

Recently, we have overcome these discovery challenges through a novel method to discern gLSNe Ia in wide-field optical surveys (Goldstein & Nugent 2017). We consider the strong gravitational lensing of SNe Ia by quiescent (E/S0) galaxies, which have three properties that are useful to identify strongly lensed SNe Ia. First, normal SNe Ia are the brightest type of supernovae that have ever been observed to occur in quiescent galaxies. Second, the absolute magnitudes of normal SNe Ia in quiescent galaxies are remarkably homogeneous, even without correcting for their colors or light curve shapes. Finally, due to the sharp 4000 angstrom break in their spectra, quiescent galaxies tend to provide accurate photometric redshifts from large-scale multicolor galaxy surveys such as the Sloan Digital Sky Survey, DECaLS and in the future LSST. A high-cadence, wide-field imaging survey can leverage these facts to systematically search for strongly lensed SNe Ia in the following way. Given the photometric redshift, compute the absolute brightness of the SN in the quiescent galaxy and if it is brighter than the normal population of SNe Ia which should occur there, it is likely a background SN Ia being lensed by the quiescent galaxy. This method has been refined even further to include not only the brightness of the supernova, but the shape of the light curve given the photometric redshift (Goldstein et al. 2018b).

An important property of this search technique is that it does not require the ability to resolve the lensed images to perform discovery. Once lensed SN Ia candidates are identified, they can be confirmed using high-resolution imaging, e.g., Laser Guide Star Adaptive Optics or space-based imaging such as the *Hubble Space Telescope* (*HST*) or, in the future, by the *James Webb Space Telescope* (*JWST*) and the *Wide Field Infrared Space Telescope* (*WFIRST*).

Given the nominal ZTF survey design coupled with stacking the proprietary data over a ten-day baseline, the detailed Monte Carlo simulations of Goldstein et al. (2018a) show that we would find ~ 8.6 gLSNe (of all types) per year, of which approximately 1.2 are Type Ia, 2.8 are Type IIP, 0.3 are Type IIL, 0.4 are Type Ib/c, 0.2 are SN 1991T-like, and at least 3.8 are Type IIn, consistent with the calculations of Tonry

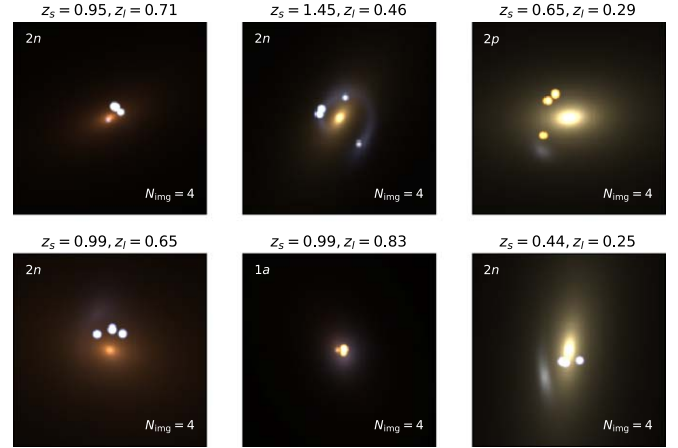


Figure 5. Noiseless $6'' \times 6''$ composite *gri* images of 6 simulated gLSNe, their lens galaxies, and their lensed host galaxies, “detected” by ZTF in the simulations of Goldstein et al. (2018a). Each image is “taken” exactly one night after the transient is detected as a gLSN candidate based on a light-curve fit to the simulated ZTF data. The FWHM of the seeing on the images is $0''.1$, and the pixel scale is $0''.04$, identical to that of the UVIS channel of the Wide Field Camera 3 (WFC3) on *HST*.

(A color version of this figure is available in the online journal.)

(2011) for gLSNe Ia in the ATLAS survey. Some examples of these simulated systems are shown in Figure 5. These lens systems comprise both doubles and quad systems (like iPTF16geu; Goobar et al. 2017) in a ratio of 2:1 due to the nature of the discovery mechanism. The discovered gLSNe have a median $z_s = 0.8$, $z_l = 0.35$, $\mu_{\text{tot}} = 30$, $\Delta t_{\text{max}} = 10$ days, $\min(\theta) = 0''.25$, and $N_{\text{img}} = 4$.

7. AGN and TDEs

While searches for supernovae and similar explosive phenomena tend to avoid the cores of resolvable galaxies and nuclear-dominated sources, these are the sites of a variety of astrophysical phenomena that relate to the physics of accretion disks and interactions with (super)massive black holes.

7.1. Tidal Disruption Events

A class of transients associated with the nuclei of galaxies is tidal disruption events. A TDE occurs when a star wanders close enough to a central massive black hole (MBH) to be shredded apart by tidal forces (Lidskii & Ozernoi 1979; Rees 1988). A luminous flare is observable when this distance of approach, the tidal disruption radius, is outside the event horizon of the MBH. These events are rare, with a volumetric rate a factor of 100 smaller than for SNe, with a per galaxy event rate of only 10^{-4} yr^{-1} (van Velzen 2018). The rise time of a TDE is of particular importance, as it scales as $M_{\text{BH}}^{1/2}$ (Lodato et al. 2009; Guillochon & Ramirez-Ruiz 2013), and can be used as a probe for dormant MBHs otherwise

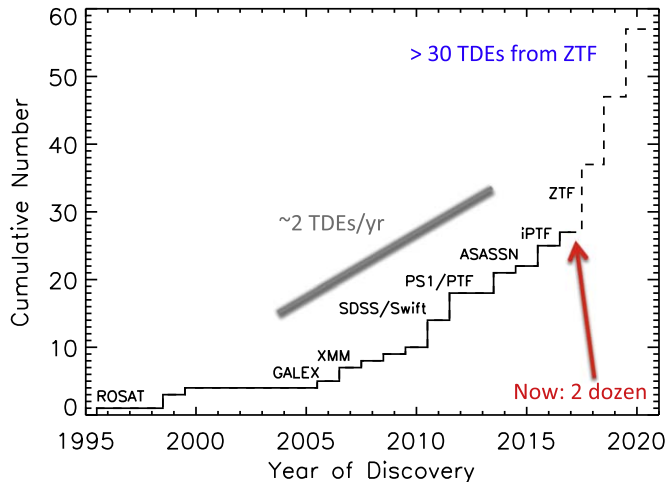


Figure 6. Cumulative discovery rate of tidal disruption events as a function of time, with the onset of new surveys labeled. Note the dramatic predicted jump in discovery rate from ~ 2 TDEs per year, to ~ 10 bright, early TDE discoveries by ZTF with SEDM spectroscopic classification per year.

(A color version of this figure is available in the online journal.)

unobservable in distant galaxies. However, there are only about a dozen TDEs with well-sampled light curves in the literature (see review by (Hung et al. 2017)), and only a few with pre-peak light curves. After peak, the bolometric luminosity is expected to follow the fallback rate of the bound stellar debris, which declines as a $t^{-5/3}$ power-law (Rees 1988; Phinney 1989; Evans & Kochanek 1989).

From a systematic study of nuclear transients from iPTF, we expect a yield of 4_{-3}^{+5} TDEs per month in the ZTF public Northern Sky Survey (Hung et al. 2018; see Figure 6). Of these TDEs, we expect $\sim 20\%$ to have peak magnitudes < 19 mag, bright enough for classification with SEDM, and discovered on the rise to peak. The selection of TDE candidates will greatly benefit from the $g - r$ color measured by ZTF with g and r observations on the same night, and the measurement of the relative offset of the transient to the host galaxy in the reference image. TDEs are bluer and have less color evolution than SNe (van Velzen et al. 2011; Hung et al. 2018), and the majority of AGN can be removed from catalog matches and previous variability history. Spectroscopic follow-up and UV and X-ray follow-up imaging will be used for classification purposes. TDEs are characterized by broad helium and/or hydrogen emission lines, a blue, UV-bright continuum, and soft X-ray emission. A large sample of well-sampled g and r TDE light curves from ZTF, in particular those with a pre-peak discovery, will be critical for mapping the properties of the TDEs to their host galaxy properties and central black hole demographics.

The rate of TDEs depends on the rate at which stars are scattered into the “loss cone” of the MBH, the region of phase space for which a star’s orbit passes within the tidal disruption radius, and is a sensitive probe of the nuclear stellar structure of

galaxies (Stone & van Velzen 2016). The TDE rate can also be an important probe of MBH demographics, with a potential dependence on the mass of the MBH (Wang & Merritt 2004), the presence of a binary MBH (Chen et al. 2011) or recoiling coalesced MBH (Stone & Loeb 2011), and the MBH occupation fraction (Stone & Metzger 2016). With a statistically significant sample of TDEs from ZTF, we can measure the rates of TDEs as a function of black hole mass and host galaxy type, and look for these theoretically predicted dependencies.

7.2. Active Galactic Nuclei

Variability is a ubiquitous property of unobscured active galactic nuclei. In particular, Sesar et al. (2007) showed that $> 90\%$ of type 1 quasars showed optical variability above a level of 2% in the 290 deg² SDSS Stripe 82 survey on a timescale of several years. Scaling up to the area of the ZTF public survey, which has a comparable depth of $r \sim 20.5$ mag, we should detect \sim half a million variable AGN. About 1 in 10,000 of these fall into the category of extreme variable AGN (Graham et al. 2017) showing significant flaring activity over months to years or other distinct patterns of variability. These may be related to stellar phenomena in the accretion disk or gravitational microlensing.

With its large survey volume, ZTF will also have the capability to catch AGN in the act of “changing look” from a narrow-line (type 2) to a broad-line (type 1) spectrum (Shappee et al. 2014; LaMassa et al. 2015) and vice versa. With iPTF, we were able to use the detection of a nuclear transient in an SDSS LINER galaxy to trigger follow-up optical spectroscopy and *Swift* UV and X-ray imaging to reveal that the galaxy had transformed into a broad-line quasar in < 1 yr (Gezari et al. 2017). The rate of changing-look AGN (CLAGN) is not yet well constrained; however, from a pilot study of spectroscopic follow-up of nuclear transients in iPTF from type 2 AGN, we expect ~ 10 per year with ZTF. Constraining the turn-on/turnoff timescale for CLAGN is important for constraining the mechanism responsible for their spectral transformation.

One of the challenges in detecting these types of events is that the detection timescale from difference imaging can be several months into the phenomenon—the day-to-day variability is gradual, so it takes quite some time before the change has become significant enough relative to a reference image to be detected. Fortunately, decade baseline archives of AGN variability over most of the sky are now available, e.g., CRTS (Drake et al. 2009), PTF (Law et al. 2009), and ATLAS (Tonry et al. 2018), so that the historical behavior of the sources ZTF will see can be characterized and modeled, although the optimal way to combine data from multiple surveys to maximize the information content still needs to be determined. The expected variability can then be predicted, either for a given night or over a particular timeframe, and compared with

what is observed. In this way, significant changes from the forecast variability can be identified more quickly and earlier follow-up of the activity, be it changing-look, flaring or something else, triggered. Our models suggest that we can track ~ 50 AGN per year in this manner, giving valuable insights into accretion disk mechanics.

8. Stellar Variability

Variable stars show up in very different flavors ranging from ultra-short period objects like pulsating white dwarfs or ultracompact binaries with periods as short as minutes up to objects with periods of months to years like Cepheid or Mira variables. Over the last two decades, many surveys have increased our knowledge in variable stars significantly. These surveys include the Optical Gravitational Lensing Experiment (OGLE; e.g., Soszyński et al. 2015), CRTS (Drake et al. 2009), PTF (Law et al. 2009), the Vista Variables in the Via Lactea (VVV; Saito et al. 2012), ASAS-SN, (Shappee et al. 2014), and most recently, ATLAS (Heinze et al. 2018).

In the transient sky, we expect phenomena including outbursts of young stellar objects, M-star flares, and Nova/dwarf nova eruptions. Archival light curves will allow us to study pulsating and rotating stars, as well as compact binaries. Down to a limiting magnitude of 20.5–21 with a median FWHM of ≈ 2 arcsec, ZTF will provide one of the best data sets for time-domain astronomy in the Northern hemisphere at low Galactic latitudes, with a median of about ≈ 150 epochs per year at a cadence of minutes to days.

The paradigm of star formation now explicitly includes the concept of episodic accretion. Stars are thought to accumulate some fraction of their mass in the initial spherical infall stage, some fraction during early-stage disk accretion that is punctuated by periods of elevated accretion, and finally the last remaining few to 10% of their final mass during the optically visible stage of pre-main-sequence evolution, which is characterized by mostly low disk accretion rates but also by infrequent bursts. Among the bursts, the most extreme type, called FU Ori events, last decades to perhaps centuries, and involve a thermal or a (gravo-) magneto-rotational instability in the inner ~ 1 au of the disk. Bursts with smaller amplitude and shorter duration (months to year-long), called EX Lup type events, may be related to instabilities associated with the interaction region between the disk and the stellar magnetosphere. Outside of the bursts, during routine low-state accretion phases, young star photometric variability occurs with amplitudes between about 2%–20% and on timescales of 1–2 days, with quite diverse light curve shapes. Recent space-based work with CoRoT, *MOST*, and K2 have illuminated heterogeneity, but also the patterns, characterizing the low-state accretion in young stars. However, the discovery and study of the more rare EX Lup and FU Ori events, including secure determination of their occurrence rates, remains the domain of

wide-field, moderate-cadence, long-duration photometric surveys like ZTF.

(Ultra)compact binaries are a rare class of binary systems with periods below a few hours (detached or semi-detached), consisting of at least one compact object. The study of (ultra)compact binaries is important to our understanding of such diverse areas as supernova Type Ia progenitors and binary evolution, and they are predicted to be the strongest gravitational-wave sources in the LISA band. Because (ultra)compact binaries show up in light curves with variations on timescales of the orbital period (e.g., due to eclipses or tidal deformation of the components), ZTF is well suited to identify (ultra)compact binaries in a homogeneous way. We expect that the majority of the periodic objects will be typical pulsating stars like Delta Scuti pulsators. The key will be to find the needle in the haystack and select the (ultra)compact systems from the bulk of pulsating stars. A combination of color-selection, proper motions and distances will allow us to distinguish between the bulk of pulsators with potential (ultra)compact binaries, like double white dwarfs, cataclysmic variables (CVs) or hot subdwarf binaries. Among the most numerous CVs will be the large amplitude eruptions of the oldest, lowest mass transfer dwarf novae, allowing a study of the CV graveyard. The large number (≈ 1000 s) of expected (ultra)compact binaries discovered by ZTF will allow us to provide an empirical space density for different types of compact post-common envelope binaries in the Galaxy. The expected large sample will challenge common envelope and binary evolution theories (e.g., predicted versus observed orbital period and component mass distributions).

Multicolor light curves of eclipsing binary stars allow us to study their stellar parameters in great detail. The duration, depth, and shape of the eclipses allows us to determine the relative stellar radii and temperature ratio. We will systematically search the ZTF light curves for eclipsing systems, and use the ZTF g , r , and i light curves, combined with colors and distances, to determine the system parameters of all eclipsing binaries observed by ZTF. The size of the sample allows us to systematically study the populations of different binary stars. Specifically, we can measure the space density and properties of binary systems that experienced stable or unstable mass transfer. The eclipsing binary sample should also contain rare eclipsing systems. Examples are EL CVn binary stars, eclipsing brown dwarfs, and eclipsing WD systems. In addition, ZTF data also allows us to detect or set an upper limit to the rate of planets around white dwarfs (Agol 2011) and large planets around M-dwarf stars (e.g., Bayliss et al. 2018).

Be stars are extreme rotating main-sequence objects that at least once show $H\alpha$ emission line in the spectrum. Moreover, they are also known as photometric variables. In a sample of 289 Be stars, Hubert & Floquet (1998) reported that nearly half of them show some photometric variability and, based on the Hipparcos catalog (ESA 1997), an almost entire sample of

early Be stars are variables. A diversity of variability can be found among the Be stars, including non-radial pulsation, intermediate periodicity, long-term variation, semi-regular outburst and outburst variation (Labadie-Bartz et al. 2017). The origin of these variabilities, or so-called the Be phenomenon, remains elusive. One possible mechanism is the instability of the accretion disk (Rivinius et al. 2013). However, the main challenge in the Be phenomenon is their wide variety of variabilities which required high-cadence sampling rate with monitoring over years. Therefore, most studies of Be phenomenon are on the bright end ($r < 13.5$ mag). Given its combination of ultra wide-field, high cadence and multi-year observations, ZTF provides an opportunity to investigate the Be phenomenon for faint Be stars ($r > 13.5$ mag), especially those found by IPHAS (Raddi et al. 2015), as well as the recent Be candidates selected by PTF (Yu et al. 2018) and LAMOST (Lin et al. 2015).

9. Small Solar System Bodies

Small solar system bodies are remnants of the formation stage of the solar system. They encompass all comets and asteroids, Trojans, Centaurs, near-Earth objects (NEOs) and trans-Neptunian objects. Studies of small bodies contribute to the understanding of several fundamental questions in planetary science, such as the composition of the proto-planetary disk, the evolutionary history of the solar system, as well as the transportation and distribution of water and organic materials in the solar system. Time-domain studies of small bodies include their discovery, behavior monitoring, and the detection and rapid follow-up of transient events. The advent of all-sky surveys such as Pan-STARRS, the Catalina Sky Survey, LINEAR, and NEAT have resulted in more small body discoveries at increasingly larger distances from the Sun (Galache et al. 2015; Meech et al. 2017). Among current surveys (c.f. (Jedicke et al. 2015a)), the Zwicky Transient Facility will provide a combination of broad and fast coverage. It will also serve as a precursor to small body observation with LSST (Schwamb et al. 2018), testing the piggyback mode of NEO discovery and operations of mini-surveys.

9.1. Discovery

Survey and discovery of NEOs is the critical first step for hazard assessment as well as scientific research. The cumulative efforts of the past few decades have discovered >95% of kilometer-sized NEOs; however, it is estimated that the coverage of smaller NEOs is less than 10% complete below 200 meters and less than 2% complete below 100 meters (e.g., Jedicke et al. 2015b). Events like the 2013 Chelyabinsk impact (Brown et al. 2013) clearly demonstrated the hazard posed by small asteroids. Such asteroids are typically faint and only become visible when they approach Earth, at which time the “trailing loss” effect begins to occur (e.g., Harris &

D’Abramo 2015). The trailing loss presents a challenge for conventional moving object detection algorithms which are tuned to detect point-like sources. For a typical NEO geocentric velocity of 20 km s^{-1} , a survey resolution of 1 arcsec, and an exposure time of 30 s, the geocentric distance that trailing loss starts to become significant is about 0.1 au.

Part of the ZTF NEO discovery effort will be built on the exploratory research done by Waszczak et al. (2017), who developed and optimized a pipeline for the detection of trailed NEOs in real-time PTF images. This pipeline is being optimized to enable effective real-time detection of trailed NEOs in ZTF images. ZTF has also deployed a pipeline dedicated to the detection of point-like moving objects (Masci et al. 2017) to cover the non-trailed moving objects.

The ZTF NEO discovery effort is mainly piggybacked to other surveys, with the exception of the Twilight Survey, a mini-survey that is designed to repeatedly survey the regions with small solar elongation. The goal is to explore interesting phenomena that happen inside Earth’s orbit, including various Sun-approaching comets (e.g., Knight et al. 2010; Ye et al. 2014; Hui et al. 2015); the asteroid population that is predicted to be thermally disrupted (Granvik et al. 2016); the poorly understood population of Earth Trojans and temporarily captured natural satellites (Connors et al. 2011; Bolin et al. 2014), and NEOs approaching Earth from the direction of the Sun like the Chelyabinsk event.

All astrometric measurements of trailed and non-trailed moving objects will be submitted to the Minor Planet Center (MPC) in the new Astrometry Data Exchange Standard (ADES) format.⁴² The MPC will serve as the liaison for international follow-up observers. ZTF will use its self-follow-up mode on the P48 system to confirm both ZTF-discovered NEOs and to participate in clearing the MPC’s NEO Confirmation Page.

9.2. Characterization

Cometary activity varies with heliocentric distance. Upon approach to the Sun, the temperature of the surface and immediate subsurface is raised, causing ices to sublimate, depending on their proximity to the surface and composition (Meech & Svoren 2004; Prialnik et al. 2004). Therefore, a comet’s coma may change composition as it orbits the Sun. In addition, the seasonal context of the nucleus affects which surface areas receive sunlight, and provides another means for coma variability. Variations of coma brightness (i.e., activity) and color (i.e., composition) thus provides a means of exploring heterogeneities of comet nuclei. We predict that ZTF can detect at least 30 comets per night ($V < 21$), and many of those comets will be observable for periods longer than a

⁴² <https://minorplanetcenter.net/iau/info/ADES.html>

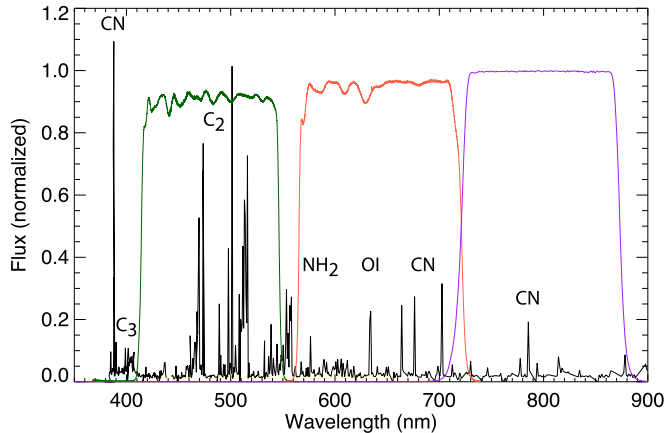


Figure 7. Using filter imaging ZTF will be able to monitor the gas and dust content of cometary comae. Here, we show the transmission of the ZTF *g* (green, left), *r* (red, center), and *i* (purple, right) filters, superimposed on the spectrum of gas-rich comet 122P/De Vico (Cochran & Cochran 2002). The *g* filter contains the emission of C_2 molecules, whereas the other filters are mostly free of cometary emission lines. The signal in the *r* and *i* filters will come mostly from sunlight reflected by dust surrounding the nucleus.

(A color version of this figure is available in the online journal.)

year. Depending on sky conditions, comet brightness, and background, we anticipate a photometric accuracy of 0.1 mag.

Our photometry methods allow us to use ZTF to systematically produce accurate comet light curves. As is shown in Figure 7, images acquired in different filters can be used as a diagnostic of the comet’s dust-to-gas ratio over time; the *g* filter contains bright emission lines of C_2 molecules, whereas the *r* and *i* bandpasses are mostly free of cometary emission features and thus sample sunlight reflected by dust in the coma.

Asteroid light curves can be used to measure several fundamental properties for asteroids, such as shape, spin status, and taxonomy. The statistics of asteroid rotations can help to understand how their evolution is affected by mutual collisions, gravitational perturbations of planets, and the YORP effect. Phase functions can be used to determine asteroid taxonomy. Combining rotation period and taxonomy, we are also able to study the spin-rate limits for different type asteroids, which is a proxy of asteroid bulk density (Chang et al. 2015). We expect to collect $\sim 100,000$ asteroid light curves per year, from which we will be able to derive rotation periods and phase functions.

Most asteroids are gravitationally bounded aggregations (“rubble-piles”). It is thought that rubble-pile asteroids cannot have rotation periods less than a critical limit, (i.e., the 2.2 hr spin-rate limit (Harris 1996)) or they will disintegrate. However, it has been found that a small number of asteroids have rotation periods shorter than this limit, implying that they may have different structure from the average asteroid. PTF has discovered three of the six super-fast rotators (SFRs) known to date (Chang et al. 2017; Waszczak et al. 2015 and the references therein). However, the detection rate is still too low

to place a meaningful constraint to the SFR population. With its large sky coverage, ZTF can improve our knowledge to the SFR population.

The binarity of asteroids probes the solar system collisional evolution (e.g., Pravec et al. 2010) and measures the dynamical mass of asteroids. A possible method for searching for binary asteroids and measuring their mass is via looking for astrometric variations from a pure Keplerian orbit. This method is currently being tested on PTF data (Polishook & Ofek, 2019, in preparation). Given the large number of asteroid images we expect to acquire with ZTF, this simple method may enable us to find most binary asteroids (and Kuiper Belt objects) in the solar system.

9.3. Transient Events

The systematic, high-cadence monitoring of small solar system bodies will provide a baseline that allows ZTF to find transient events such as cometary outbursts and fragmentation events (Ye et al. 2015; Ishiguro et al. 2016), collisions between asteroids (Snodgrass et al. 2010; Bodewits et al. 2011), unexpected or irregular activity in asteroids (Jewitt 2012; Waszczak et al. 2013; Ye 2017) and Centaurs (Jewitt 2009). The cadence of the ZTF observations will allow us to evaluate the frequency of these events. The early discovery of such transient events enables rapid follow-up observations which are critical for the characterization of these events, because the ejected material quickly sublimates or dissipates away.

10. Astroinformatics and Astrostatistics

ZTF is well positioned to enable the fields of astroinformatics and astrostatistics make significant strides through the development and testing of novel computational and statistical methodologies related to large data sets. These new algorithms and techniques will not only be useful for analyzing ZTF data, but will also provide a ready-to-use analysis toolkit for data from future surveys like LSST. Indeed, the anticipation of ZTF data has already led to the development of new data-processing pipelines by *IPAC* (Masci et al. 2019) and the implementation of the Kafka system (Patterson et al. 2019).

ZTF data will necessitate new statistical methodologies and machine learning algorithms specifically designed for astronomy and astrophysics. In particular, methods for time series analysis and populations studies that allow testing and comparison of physical models are needed. Additionally, reliable classification algorithms will be needed to properly perform scientific inference. Finally, model comparisons using modern statistical methods will be fundamental in ruling out physical models in light of complex ZTF data.

As large data sets from projects such as ATLAS, ASAS-SN, CRTS, Gaia, *JWST*, LSST, Pan-STARSS, etc. continue to become available into the 2020s and 2030s, there will be a demand for statistical and computational methodologies which

not only handle large amounts of data but also extract the most information possible. ZTF is unique in that, combined with its follow-up network, it will provide one of the first opportunities to develop and test methods for large data sets that have significant temporal information.

10.1. Population Studies

ZTF will discover many faint and fast-evolving transients, allowing a search for subpopulations and tests of proposed physical mechanisms behind these phenomena (Section 3.6). ZTF will also provide us with an unbiased and complete sample of SNe Ia within $z < 0.1$, which in turn will allow us to investigate the effects of host environments (Section 5). In both of these cases, studying the population of light-curve data is key to identifying patterns and subpopulations. Thus, modern cluster-finding algorithms for time series data are needed to analyze the light curves of these transients.

Methods for time series clustering exist in other research areas such as statistics, finance, medicine, and economics, but not all of these new methods have made it to astronomy (for a review of time series clustering methods, see Aghabozorgi et al. 2015). Recurring challenges for time series clustering methods include how to deal with missing data and the reliance on mathematical distance measures. Recently, new methods have been proposed that overcome these challenges (e.g., Wang et al. 2006) and these could be useful for the analysis of ZTF light-curve population studies. At the same time, astronomical time series of transient sources bring new challenges to the table—for example, uncertainties in distance to the source and how to account for reddening due to dust.

The curve data sets of specific populations (such as SE SNe and SNe Ia) will present an opportunity for astroinformatics and astrostatistics to bring in methods from other research areas to make discoveries, and to build upon and tailor these techniques for astronomy.

10.2. Classification

Classification of one form or another will lie at the heart of solving many of the ZTF science cases. The sheer number of sources and alerts from ZTF will necessitate reliable classification tasks with little human intervention. Over the past twenty years or so, the proliferation of algorithms in the field now called machine learning has led to the creation of a powerful toolbox of methods that can perform classification in a large variety of different contexts. The challenge here lies in the structure of both the problems to be addressed and the data itself.

In some instances, correctly predicting the source or alert type may be all that is required, but the ultimate goal of most classification tasks in the context of ZTF is scientific inference. For example, when classes of sources are identified with the goal of performing the population studies mentioned above,

biases within the classified data set must be carefully assessed and propagated through to the inference stage. Achieving the latter is not always straightforward with many of the newer deep learning methods, although recent developments related to (local) interpretability (e.g., Ribeiro et al. 2016; Krause et al. 2016) and probabilistic machine learning (e.g., Tran et al. 2016; Ghahramani 2015) may be able to either shed light on these biases or incorporate them directly into the subsequent modeling tasks.

In contrast to data sources often considered in machine learning contexts, the data derived from the ZTF survey will be very heterogeneous, unevenly sampled, and subject to occasionally catastrophic outliers. Moreover, the data will include variable uncertainties. Recent work shows a range of different approaches for dealing with such issues. Promising results are found through methods such as recurrent neural networks (Naul et al. 2018), convolutional neural networks trained on two-dimensional representations of light curves (Mahabal et al. 2017), and the use of deep neural networks for phenomenological discovery of variable star classes (Heinze et al. 2018).

The peculiarities of the ZTF data—combined with the requirement to classify sources and subsequently perform inference—implies that standard techniques may not deliver the performance necessary to answer the scientific questions in this paper. However, these constraints also present an opportunity to develop new classification methods that can be carried forward to future surveys that share the same challenges.

In addition to the real-bogus separation covered in Mahabal et al. (2019), we identify three objectives for classification with ZTF data: classification for follow-up, classification for scientific inference, and finding the unexpected. Each objective presents its own challenges. Below, we show where recent research from other domains could be usefully applied to ZTF data or where new methods must be developed to overcome these challenges.

With a projected one million alerts per night, ZTF will produce a large number of transients. Because observing time is scarce and expensive, there is significant impetus to optimize which sources should be followed up with other facilities, and how soon they should be observed to maximize scientific output. Any algorithm must be capable of dealing with a continuously changing data set on top of the heterogeneity mentioned above, and be able to update predictions almost on-the-fly, for example as part of an alert brokering system (e.g., ANTARES; Narayan et al. 2018). There is a wealth of methods related to active learning (i.e., learning with feedback; Ishida et al. 2019; Vilalta et al. 2017; Peng et al. 2017; He et al. 2015) and Online Learning (i.e., learning from evolving data streams; Aggarwal 2007; Nguyen et al. 2015) that can be tested with ZTF in order to both enable follow-up studies as well as prepare for future surveys. These approaches may be combined

with other techniques (e.g., probabilistic forecasting techniques, see Kuznetsov & Mohri 2015, for an example) in order to estimate when a future follow-up observation should be taken. Only by optimizing the information gathered about the source can competing models be rigorously tested. Owing to the data volume, methods deployed on clusters, GPUs, and other multi-processing hardware will find increasing use (e.g., Gieseke et al. 2015, 2017).

As mentioned above, many science cases rely heavily on identifying a complete subset of the relevant source type (e.g., for SN Ia cosmology, see also Section 5). A key challenge in identifying a complete subset with machine learning is the dearth of complete, applicable training data sets for which the truth is known. One option is to simulate data sets for a given instrument, but the correctness of the derived prediction depends crucially on the assumption that the simulated training data matches the real test data exactly. Many algorithms, especially more modern deep learning frameworks, tend to be extremely vulnerable to mismatches between training and test data (e.g., Evtimov et al. 2017). Recent advances in the field of transfer learning may make it possible to use training data sets generated with other surveys and use the information in them to generate accurate classifications for ZTF sources (Aswolinskiy & Hammer 2017; George et al. 2018).

In addition, the field of probabilistic machine learning has recently received much attention from within the computer science community. Different domains have seen an emergence of time series methods within a probabilistic framework, within machine learning (e.g., to model motion capture data (Ainsworth et al. 2018), housing prices (Glynn & Fox 2017) or homelessness (Ren et al. 2017)). These methods align well with the science goals of ZTF, and will allow for direct propagation of uncertainties and biases into the resulting astronomical inferences. However, even with transfer learning, there might not exist a complete, unbiased training data set for ZTF, in which case unsupervised methods (see below) may present a better solution.

Serendipity has traditionally been a strong component of astronomical discovery, especially when the instrument in question opens up a new part of parameter space. In addition, some science cases have no strong prior on the number or types of classes. Much of the work within the machine learning community has focused on supervised machine learning. However, finding the unknown with traditional supervised methods is exceedingly difficult. Here, new approaches to unsupervised machine learning may help us discover unknown transients and new source classes. In particular, the recent development of methods for the classification of sparse, irregularly sampled time series based on Gaussian Processes (e.g., Li & Marlin 2016; Ghassemi et al. 2015), deep learning (e.g., Lipton et al. 2016; Che et al. 2018) and time series clustering have shown promise across multiple domains.

11. Summary

In this paper, we have summarized the main science drivers that led to the Zwicky Transient Facility (ZTF) consisting of a 47 deg² imager on the Palomar 1.2-m Oschin (Schmidt) telescope and a low-resolution spectrometer, the Spectral Energy Distribution Machine (SEDM), on the Palomar 60-inch telescope. From cometary outbursts and asteroid collisions to infant SNe and failed GRB jets, from Be stars and ultracompact binaries to interactions with (supermassive) black holes, populations of transient and variable astrophysical sources can now be studied in great detail. Although comprehensive, this list is not exhaustive and the ZTF public alert stream offers the community ample opportunity to make their own discoveries.

The rates of potential discoveries—supernovae and asteroids every night, a changing-look AGN every week, a TDE every month, a gravitationally lensed SN every quarter, and maybe a few unexpected transients a year, with each easily followed-up spectroscopically by a 5–10 m class telescope (and smaller for photometry) take us into the new territory of deciding each night what the most interesting sources currently are and whether the previous night’s sources still merit continued attention. This problem will become acute once even more powerful facilities come online, in particular, LSST. Even with our considerable follow-up resources we are not in a position to follow *all* transients identified with ZTF. We call this problem the conundrum of abundance.

To start with abundance is good, particularly for astronomy that depends primarily on photometric data. For instance, consider the search for rare types of variable stars (e.g., double degenerates with very short periods). The larger the data set, the higher the chance of discovery. Large data sets also allow the extraction of huge samples of ordinary phenomena (e.g., RR Lyrae stars) and large samples could lead to identification of finer sub-classes.

The conundrum of abundance is a problem for transient object science in which follow-up is needed.⁴³ A million alerts per night ensures that the sky is always saturated with follow-up targets (from NEOs to TDEs), enabling us to select and focus on the ones most likely to yield the highest value results (depending on a group’s area of interest). The solution is to sharply define science programs that can be undertaken with existing facilities. This would mean designing filters that efficiently find desired transients while suppressing false positives. In fact, in this respect, we have already achieved good performance in the area of SLSNe, TDEs and relativistic transients. Bright transients will always remain interesting. Given the success of the SEDM, we advocate similar low-resolution spectrographs for 2-m class telescopes.

⁴³ For well-behaved transients such as Type Ia, a purely photometric approach using photometric redshifts for host galaxies is certainly feasible.

Finally, the night sky is finite in extent and with multiple facilities scanning the same regions every night, there is clearly scope for synergies to optimize scientific discovery. A key component of this has to be adequate community infrastructure and coordination to support the real-time distribution, characterization, and classification of million of alerts per night from surveys (let alone follow-up observations of interesting sources), as well as systematic searches of archives of billions of time series. ZTF is clearly a pathfinder for some of this and coordinated efforts across surveys drawing on it will create the basis for LSST and other time-domain surveys of the next decade and beyond.

Based on observations obtained with the Samuel Oschin 48-inch Telescope and the 60-inch Telescope at the Palomar Observatory as part of the Zwicky Transient Facility project, a scientific collaboration among the California Institute of Technology, the Oskar Klein Centre, the Weizmann Institute of Science, the University of Maryland, the University of Washington, Deutsches Elektronen-Synchrotron, the University of Wisconsin-Milwaukee, and the TANGO Program of the University System of Taiwan. Further support is provided by the U.S. National Science Foundation under grant No. AST-1440341.

J. Sollerman acknowledges support from the Knut and Alice Wallenberg Foundation.

E. Ofek is grateful for support by a grant from the Israeli Ministry of Science, ISF, Minerva, BSF, BSF transformative program, and the I-CORE Program of the Planning and Budgeting Committee and The Israel Science Foundation (grant No. 1829/12).

A. Gal-Yam is supported by the EU via ERC grant No. 725161, the Quantum Universe I-Core program, the ISF, the BSF Transformative program and by a Kimmel award.

S. Gezari is supported in part by NSF CAREER grant 1454816 and NSF AAG grant 1616566.

C.-K. Chang, W.-H. Ip, C.-D. Lee, Z.-Y. Lin, C.-C. Ngeow, and P.-C. Yu thank the funding from Ministry of Science and Technology (Taiwan) under grant 104-2923-M-008-004-MY5, 104-2112-M-008-014-MY3, 105-2112-M-008-002-MY3, 106-2811-M-008-081, and 106-2112-M-008-007.

M. Bulla and A. Goobar acknowledge support from the Swedish Research Council (Vetenskapsrådet) and the Swedish National Space Board.

E. Bellm, B. Bolin, A. Connolly, V. Z. Golkhou, D. Huppenkothen, Z. Ivezić L. Jones, M. Juric, and M. Patterson acknowledge support from the University of Washington College of Arts and Sciences, Department of Astronomy, and the DIRAC Institute. University of Washington's DIRAC Institute is supported through generous gifts from the Charles and Lisa Simonyi Fund for Arts and Sciences, and the Washington Research Foundation. M. Juric and A. Connolly acknowledge the support of the Washington Research

Foundation Data Science Term Chair fund, and the UW Provost's Initiative in Data-Intensive Discovery.

E. Bellm, A. Connolly, Z. Ivezić L. Jones, M. Juric, and M. Patterson acknowledge support from the Large Synoptic Survey Telescope, which is supported in part by the National Science Foundation through Cooperative Agreement 1258333 managed by the Association of Universities for Research in Astronomy (AURA), and the Department of Energy under contract No. DE-AC02-76SF00515 with the SLAC National Accelerator Laboratory. Additional LSST funding comes from private donations, grants to universities, and in-kind support from LSSTC Institutional Members.

B.T. Bolin acknowledges funding for the Asteroid Institute program provided by B612 Foundation, W.K. Bowes Jr. Foundation, P. Rawls Family Fund, and two anonymous donors in addition to general support from the B612 Founding Circle.

M.T. Soumagnac acknowledges support by a grant from IMOS/ISA, the Ilan Ramon fellowship from the Israel Ministry of Science and Technology and the Benozio center for Astrophysics at the Weizmann Institute of Science.

A. A. Miller is funded by the Large Synoptic Survey Telescope Corporation in support of the Data Science Fellowship Program.

J. Bauer, T. Farnham, and M. Kelley gratefully acknowledge the NASA/University of Maryland/MPC Augmentation through the NASA Planetary Data System Cooperative Agreement NNX16AB16A.

M. M. Kasliwal and Q.-Z. Ye acknowledge support by the GROWTH (Global Relay of Observatories Watching Transients Happen) project funded by the National Science Foundation PIRE (Partnership in International Research and Education) program under Grant No 1545949.

A. A. Mahabal acknowledges support from the following grants: NSF AST-1749235, NSF-1640818, and NASA 16-ADAP16-0232.

M. W. Coughlin is supported by the David and Ellen Lee Postdoctoral Fellowship at the California Institute of Technology.

S. Ghosh acknowledges the NSF award PHY-1607585.

M. Rigault acknowledges funding from the European Research Council (ERC) under the European Union's Horizon 2020 research and innovation programme (grant agreement No. 759194—USNAC).

Facilities: PO:1.2 m, PO:1.5m.

ORCID iDs

Matthew J. Graham  <https://orcid.org/0000-0002-3168-0139>
Eric C. Bellm  <https://orcid.org/0000-0001-8018-5348>

References

- Aartsen, M. G., Abraham, K., Ackermann, M., et al. 2015, *ApJ*, 809, 98
Aartsen, M. G., Abraham, K., Ackermann, M., et al. 2017a, *ApJ*, 835, 151

- Aartsen, M. G., Ackermann, M., Adams, J., et al. 2015, *ApJ*, **807**, 46
- Aartsen, M. G., Ackermann, M., Adams, J., et al. 2017b, *A&A*, **92**, 30
- Aartsen, M. G., Ackermann, M., Adams, J., et al. 2018, *Sci*, **361**, eaat1378
- Abbott, B. P., Abbott, R., Abbott, T. D., et al. 2017a, *Natur*, **551**, 85
- Abbott, B. P., Abbott, R., Abbott, T. D., et al. 2017b, *ApJL*, **848**, L13
- Abbott, B. P., Abbott, R., Abbott, T. D., et al. 2017c, *PhRvL*, **119**, 161101
- Adams, S. M., Kochanek, C. S., Gerke, J. R., Stanek, K. Z., & Dai, X. 2017, *MNRAS*, **468**, 4968
- Aggarwal, C. C. 2007, *Data Streams: Models and Algorithms*, Vol. 31 (New York: Springer Science Business Media)
- Aghabozorgi, S., Shirkhoshidi, A. S., & Wah, T. Y. 2015, *Inf. Syst.*, **53**, 16
- Agol, E. 2011, *ApJL*, **731**, L31
- Ainsworth, S., Foti, N., Lee, A. K., & Fox, E. 2018, arXiv:1802.06765
- Alexander, K. D., Margutti, R., Blanchard, P. K., et al. 2018, *ApJL*, **863**, L18
- Arcavi, I., Hosseinzadeh, G., Howell, D. A., et al. 2017, *Natur*, **551**, 64
- Aretxaga, I., Benetti, S., Terlevich, R. J., et al. 1999, *MNRAS*, **309**, 343
- Arnett, W. D. 1982, *ApJ*, **253**, 785
- Arnett, W. D., & Meakin, C. 2011, *ApJ*, **733**, 78
- Astier, P., Balland, C., Brescia, M., et al. 2014, *A&A*, **572**, A80
- Aswolinskiy, W., & Hammer, B. 2017, in Proc. of the Workshop on New Challenges in Neural Computation (NC2)
- Barkat, Z., Rakavy, G., & Sack, N. 1967, *PhRvL*, **18**, 379
- Barnes, J., Duffell, P. C., Liu, Y., et al. 2018, *ApJ*, **860**, 38
- Barone-Nugent, R. L., Lidman, C., Wyithe, J. S. B., et al. 2013, *MNRAS*, **432**, L90
- Bayliss, D., Gillen, E., Eigmlüller, P., et al. 2018, *MNRAS*, **475**, 4467
- Bellm, E. C. 2016, *PASP*, **128**, 084501
- Bellm, E. C., Kulkarni, S. R., Barlow, T., et al. 2019b, *PASP*, **131**, 068003
- Bellm, E. C., Kulkarni, S. R., Graham, M. J., et al. 2019a, *PASP*, **131**, 018002
- Berger, E. 2014, *ARA&A*, **52**, 43
- Bersten, M. C., Folatelli, G., García, F., et al. 2018, *Natur*, **554**, 497
- Betoule, M., Kessler, R., Guy, J., et al. 2014, *A&A*, **568**, A22
- Bildsten, L., Shen, K. J., Weinberg, N. N., & Nelemans, G. 2007, *ApJL*, **662**, L95
- Blagorodnova, N., Neill, J. D., Walters, R., et al. 2018, *PASP*, **130**, 035003
- Bodewits, D., Kelley, M. S., Li, J.-Y., et al. 2011, *ApJL*, **733**, L3
- Bolin, B., Jedicke, R., Granvik, M., et al. 2014, *Icar*, **241**, 280
- Briggs, M. & Fermi GBM Team 2017, APS April Meeting Abstracts, U4.007
- Bromberg, O., Nakar, E., & Piran, T. 2011, *ApJL*, **739**, L55
- Brown, P. G., Assink, J. D., Astiz, L., et al. 2013, *Natur*, **503**, 238
- Bulla, M., Goobar, A., Amanullah, R., Feindt, U., & Ferretti, R. 2018a, *MNRAS*, **473**, 1918
- Bulla, M., Goobar, A., & Dhawan, S. 2018b, *MNRAS*, **479**, 3663
- Campana, S., Mangano, V., Blustin, A. J., et al. 2006, *Natur*, **442**, 1008
- Cano, Z. 2013, *MNRAS*, **434**, 1098
- Cao, Y., Kulkarni, S. R., Howell, D. A., et al. 2015, *Natur*, **521**, 328
- Cenko, S. B., Kulkarni, S. R., Horesh, A., et al. 2013, *ApJ*, **769**, 130
- Chambers, K. C., Magnier, E. A., Metcalfe, N., et al. 2016, arXiv:1612.05560
- Chang, C.-K., Ip, W.-H., Lin, H.-W., et al. 2015, *ApJS*, **219**, 27
- Chang, C.-K., Lin, H.-W., Ip, W.-H., et al. 2017, *ApJL*, **840**, L22
- Che, Z., Purushotham, S., Cho, K., Sontag, D., & Liu, Y. 2018, *Sci. Rep.*, **8**, 6085
- Chen, X., Sesana, A., Madau, P., & Liu, F. K. 2011, *ApJ*, **729**, 13
- Chevalier, R. A., & Irwin, C. M. 2011, *ApJL*, **729**, L6
- Chugai, N. N., & Danziger, I. J. 1994, *MNRAS*, **268**, 173
- Cochran, A. L., & Cochran, W. D. 2002, *Icar*, **157**, 297
- Connors, M., Wiegert, P., & Veillet, C. 2011, *Natur*, **475**, 481
- Corsi, A., Ofek, E. O., Gal-Yam, A., et al. 2014, *ApJ*, **782**, 42
- da Cunha, E., Hopkins, A. M., Colless, M., et al. 2017, *PASA*, **34**, e047
- Danziger, I. J., & Kjaer, K. (ed.) 1991, ESO Conf. and Workshop Proc., *Supernova 1987A and Other Supernovae (Garching: ESO)*, 37
- De Cia, A., Gal-Yam, A., Rubin, A., et al. 2018, *ApJ*, **860**, 100
- De, K., Kasliwal, M. M., Cantwell, T., et al. 2018, *ApJ*, **866**, 72
- Dekany, R., Smith, R. M., Belicki, J., et al. 2016, *Proc. SPIE*, **9908**, 99085M
- Dermer, C. D., Chiang, J., & Böttcher, M. 1999, *ApJ*, **513**, 656
- Dhawan, S., Goobar, A., Mörtzell, E., Amanullah, R., & Feindt, U. 2017, *JCAP*, **7**, 040
- Dobie, D., Kaplan, D. L., Murphy, T., et al. 2018, *ApJ*, **858**, L15
- Drake, A. J., Djorgovski, S. G., Mahabal, A., et al. 2009, *ApJ*, **696**, 870
- Drout, M. R., Piro, A. L., Shappee, B. J., et al. 2017, *Sci*, **358**, 1570
- Drout, M. R., Soderberg, A. M., Mazzali, P. A., et al. 2013, *ApJ*, **774**, 58
- Ergon, M., Jerkstrand, A., Sollerman, J., et al. 2015, *A&A*, **580**, A142
- ESA 1997, ESA Special Publication, Vol. 1200, The HIPPARCOS and TYCHO catalogues. Astrometric and photometric star catalogues derived from the ESA HIPPARCOS Space Astrometry Mission
- Evans, C. R., & Kochanek, C. S. 1989, *ApJL*, **346**, L13
- Evtimov, I., Eykholt, K., Fernandes, E., et al. 2017, 1 arXiv:1707.08945
- Fabian, A. C., & Terlevich, R. 1996, *MNRAS*, **280**, L5
- Fassia, A., Meikle, W. P. S., Chugai, N., et al. 2001, *MNRAS*, **325**, 907
- Fassia, A., Meikle, W. P. S., Vacca, W. D., et al. 2000, *MNRAS*, **318**, 1093
- Feindt, U., Kerschhaggl, M., Kowalski, M., et al. 2013, *A&A*, **560**, A90
- Fernández, R., Quataert, E., Kashiyama, K., & Coughlin, E. R. 2018, *MNRAS*, **476**, 2366
- Filippenko, A. V. 1997, *ARA&A*, **35**, 309
- Flewelling, H. A., Magnier, E. A., Chambers, K. C., et al. 2016, arXiv:1612.05243
- Foley, R. J., Scolnic, D., Rest, A., et al. 2018, *MNRAS*, **475**, 193
- Foley, R. J., Smith, N., Ganeshalingam, M., et al. 2007, *ApJL*, **657**, L105
- Fraser, M., Magee, M., Kotak, R., et al. 2013, *ApJL*, **779**, L8
- Frohmaier, C., Sullivan, M., Maguire, K., & Nugent, P. E. 2018, *ApJ*, **858**, 50
- Fuller, J. 2017, *MNRAS*, **470**, 1642
- Fuller, J., & Ro, S. 2018, *MNRAS*, **476**, 1853
- Gal-Yam, A. 2012, *Sci*, **337**, 927
- Gal-Yam, A. 2017, *Observational and Physical Classification of Supernovae (Cham: Springer International)*, 195
- Gal-Yam, A., Arcavi, I., Ofek, E. O., et al. 2014, *Natur*, **509**, 471
- Gal-Yam, A., Leonard, D. C., Fox, D. B., et al. 2007, *ApJ*, **656**, 372
- Gal-Yam, A., Mazzali, P., Ofek, E. O., et al. 2009, *Natur*, **462**, 624
- Galache, J. L., Beeson, C. L., McLeod, K. K., & Elvis, M. 2015, *P&SS*, **111**, 155
- Galama, T. J., Vreeswijk, P. M., van Paradijs, J., et al. 1998, *Natur*, **395**, 670
- Gall, C., Hjorth, J., Watson, D., et al. 2014, *Natur*, **511**, 326
- Ganot, N., Gal-Yam, A., Ofek, E. O., et al. 2016, *ApJ*, **820**, 57
- Garnavich, P. M., Tucker, B. E., Rest, A., et al. 2016, *ApJ*, **820**, 23
- Gehrels, N., Cannizzo, J. K., Kanner, J., et al. 2016, *ApJ*, **820**, 136
- George, D., Shen, H., & Huerta, E. A. 2018, *PhRvD*, **97**, 101501
- Gerke, J. R., Kochanek, C. S., & Stanek, K. Z. 2015, *MNRAS*, **450**, 3289
- Gezari, S., Dessart, L., Basa, S., et al. 2008, *ApJL*, **683**, L131
- Gezari, S., Hung, T., Cenko, S. B., et al. 2017, *ApJ*, **835**, 144
- Ghahramani, Z. 2015, *Nature*, **521**, 452
- Ghassemi, M., Pimentel, M. A., Naumann, T., et al. 2015, Proc. of the Twenty-Ninth AAAI Conf. on Artificial Intelligence, 446, <https://www.aaai.org/ocs/index.php/AAAI/AAAI15/paper/view/9393/9279>
- Ghosh, S., Chatterjee, D., Kaplan, D. L., Brady, P. R., & Van Sistine, A. 2017, *PASP*, **129**, 114503
- Gieseke, F., Eugen Oancea, C., Mahabal, A., Igel, C., & Heskes, T. 2015, arXiv:1512.02831
- Gieseke, F., Polsterer, K. L., Mahabal, A., Igel, C., & Heskes, T. 2017, 2017 IEEE Symp. Series on Computational Intelligence, (SSCI), 1
- Gill, R., & Granot, J. 2018, *MNRAS*, **478**, 4128
- Glynn, C., & Fox, E. B. 2017, arXiv:1707.09380
- Goldstein, A., Veres, P., Burns, E., et al. 2017, *ApJL*, **848**, L14
- Goldstein, D. A., & Nugent, P. E. 2017, *ApJL*, **834**, L5
- Goldstein, D. A., Nugent, P. E., & Goobar, A. 2018a, arXiv:1809.10147
- Goldstein, D. A., Nugent, P. E., Kasen, D. N., & Collett, T. E. 2018b, *ApJ*, **855**, 22
- Goliath, M., Amanullah, R., Astier, P., Goobar, A., & Pain, R. 2001, *A&A*, **380**, 6
- Golkhou, V. Z., Butler, N. R., Strausbaugh, R., et al. 2018, *ApJ*, **857**, 81
- Goobar, A., Amanullah, R., Kulkarni, S. R., et al. 2017, *Sci*, **356**, 291
- Goobar, A., Dhawan, S., & Scolnic, D. 2018, *MNRAS*, **477**, L75
- Goobar, A., & Leibundgut, B. 2011, *ARNPS*, **61**, 251
- Gottlieb, O., Nakar, E., Piran, T., & Hotokezaka, K. 2018, *MNRAS*, **479**, 588
- Graham, M. J., Djorgovski, S. G., Drake, A. J., et al. 2017, *MNRAS*, **470**, 4112
- Granot, J., Guetta, D., & Gill, R. 2017, *ApJL*, **850**, L24
- Granvik, M., Morbidelli, A., Jedicke, R., et al. 2016, *Natur*, **530**, 303
- Guillochon, J., & Ramirez-Ruiz, E. 2013, *ApJ*, **767**, 25
- Hallinan, G., Corsi, A., Mooley, K. P., et al. 2017, *Sci*, **358**, 1579
- Harris, A. W. 1996, Lunar and Planetary Science Conf., **27**, 493
- Harris, A. W., & D'Abramo, G. 2015, *Icar*, **257**, 302

- He, G., Duan, Y., Li, Y., et al. 2015, 2015 IEEE XXVII International Conf. on Tools with Artificial Intelligence (ICTAI), 178
- Heinze, A. N., Tonry, J. L., Denneau, L., et al. 2018, *AJ*, **156**, 241
- Hildebrandt, H., Viola, M., Heymans, C., et al. 2017, *MNRAS*, **465**, 1454
- Ho, A. Y. Q., Kulkarni, S. R., Nugent, P. E., et al. 2018, *ApJL*, **854**, L13
- Horiuchi, S., Nakamura, K., Takiwaki, T., Kotake, K., & Tanaka, M. 2014, *MNRAS*, **445**, L99
- Hosseinzadeh, G., Sand, D. J., Valenti, S., et al. 2017, *ApJL*, **845**, L11
- Hotokezaka, K., Beniamini, P., & Piran, T. 2018, *IJMPD*, **27**, 1842005
- Howlett, C., Robotham, A. S. G., Lagos, C. D. P., & Kim, A. G. 2017a, *ApJ*, **847**, 128
- Howlett, C., Staveley-Smith, L., Elahi, P. J., et al. 2017b, *MNRAS*, **471**, 3135
- Hubert, A. M., & Floquet, M. 1998, *A&A*, **335**, 565
- Hui, M.-T., Ye, Q.-Z., Knight, M., Battams, K., & Clark, D. 2015, *ApJ*, **813**, 73
- Hung, T., Gezari, S., Blagorodnova, N., et al. 2017, *ApJ*, **842**, 29
- Hung, T., Gezari, S., Cenko, S. B., et al. 2018, *ApJS*, **238**, 15
- IceCube Collaboration 2013, *Sci*, **342**, 1242856
- Ishida, E. E. O., Beck, R., Gonzalez-Gaitan, S., et al. 2019, *MNRAS*, **483**, 2
- Ishiguro, M., Kuroda, D., Hanayama, H., et al. 2016, *AJ*, **152**, 169
- Jedicke, R., Granvik, M., Micheli, M., et al. 2015a, in *Asteroids IV*, ed. P. Michel, F. E. DeMeo, & W. F. Bottke (Tucson, AZ: Univ. Arizona Press), 795
- Jedicke, R., Granvik, M., Micheli, M., et al. 2015b, *Surveys, Astrometric Follow-Up, and Population Statistics* (Tucson, AZ: Univ. Arizona Press), 795
- Jewitt, D. 2009, *AJ*, **137**, 4296
- Jewitt, D. 2012, *AJ*, **143**, 66
- Jones, D. O., Scolnic, D. M., Foley, R. J., et al. 2018, arXiv:1811.09286
- Kaiser, N. 2004, *Proc. SPIE*, **5489**, 11
- Kasen, D. 2010, *ApJ*, **708**, 1025
- Kasen, D., & Bildsten, L. 2010, *ApJ*, **717**, 245
- Kasen, D., Metzger, B., Barnes, J., Quataert, E., & Ramirez-Ruiz, E. 2017, *Natur*, **551**, 80
- Kasliwal, M., et al. 2019, *PASP*, **131**, 038003
- Kasliwal, M. M. 2012, *PASA*, **29**, 482
- Kasliwal, M. M., Kulkarni, S. R., Gal-Yam, A., et al. 2010, *ApJL*, **723**, L98
- Kasliwal, M. M., Kulkarni, S. R., Gal-Yam, A., et al. 2012, *ApJ*, **755**, 161
- Kasliwal, M. M., Nakar, E., Singer, L. P., et al. 2017, *Sci*, **358**, 1559
- Kelly, P. L., Brammer, G., Selsing, J., et al. 2016, *ApJ*, **831**, 205
- Kelly, P. L., & Kirshner, R. P. 2012, *ApJ*, **759**, 107
- Khazov, D., Yaron, O., Gal-Yam, A., et al. 2016, *ApJ*, **818**, 3
- Kiewe, M., Gal-Yam, A., Arcavi, I., et al. 2012, *ApJ*, **744**, 10
- Kleiser, I. K. W., & Kasen, D. 2014, *MNRAS*, **438**, 318
- Knight, M. M., A'Hearn, M. F., Biesecker, D. A., et al. 2010, *AJ*, **139**, 926
- Kochanek, C. S. 2014, *ApJ*, **785**, 28
- Kochanek, C. S., Beacom, J. F., Kistler, M. D., et al. 2008, *ApJ*, **684**, 1336
- Koda, J., Blake, C., Davis, T., et al. 2014, *MNRAS*, **445**, 4267
- Köhlinger, F., Viola, M., Joachimi, B., et al. 2017, *MNRAS*, **471**, 4412
- Krause, J., Perer, A., & Bertini, E. 2016, arXiv:1606.05685
- Kulkarni, S. R., Frail, D. A., Wieringa, M. H., et al. 1998, *Natur*, **395**, 663
- Kulkarni, S. R., Perley, D. A., & Miller, A. A. 2018, *ApJ*, **860**, 22
- Kuznetsov, V., & Mohri, M. 2015, *Advances in Neural Information Processing Systems*, 541
- Labadie-Bartz, J., Pepper, J., McSwain, M. V., et al. 2017, *AJ*, **153**, 252
- LaMassa, S. M., Cales, S., Moran, E. C., et al. 2015, *ApJ*, **800**, 144
- Lamb, G. P., & Kobayashi, S. 2018, *MNRAS*, **478**, 733
- Law, N. M., Kulkarni, S. R., Dekany, R. G., et al. 2009, *PASP*, **121**, 1395
- Lazzati, D., Perna, R., Morsony, B. J., et al. 2018, *PhRvL*, **120**, 241103
- Leloudas, G., Chatzopoulos, E., Dilday, B., et al. 2012, *A&A*, **541**, A129
- Leloudas, G., Schulze, S., Krühler, T., et al. 2015, *MNRAS*, **449**, 917
- Li, S. C.-X., & Marlin, B. M. 2016, *Advances In Neural Information Processing Systems*, 1804
- Li, W.-D., Li, C., Filippenko, A. V., & Moran, E. C. 1998, *IAUC*, **6829**
- Lidskii, V. V., & Ozernoi, L. M. 1979, *SvAL*, **5**, 16
- Lin, C.-C., Hou, J.-L., Chen, L., et al. 2015, *RAA*, **15**, 1325
- Linder, E. V. 2011, *PhRvD*, **84**, 123529
- Lipton, Z. C., Kale, D., & Wetzell, R. 2016, in *Machine Learning for Healthcare Conf.*, 253
- Lodato, G., King, A. R., & Pringle, J. E. 2009, *MNRAS*, **392**, 332
- Lovegrove, E., & Woosley, S. E. 2013, *ApJ*, **769**, 109
- Lovegrove, E., Woosley, S. E., & Zhang, W. 2017, *ApJ*, **845**, 103
- Lunardini, C., & Winter, W. 2017, *PhRvD*, **95**, 123001
- Lunnan, R., Chornock, R., Berger, E., et al. 2014, *ApJ*, **787**, 138
- Lunnan, R., Chornock, R., Berger, E., et al. 2016, *ApJ*, **831**, 144
- Lunnan, R., Chornock, R., Berger, E., et al. 2018, *ApJ*, **852**, 81
- Lunnan, R., Kasliwal, M. M., Cao, Y., et al. 2017, *ApJ*, **836**, 60
- Lyman, J. D., Bersier, D., James, P. A., et al. 2016, *MNRAS*, **457**, 328
- Mahabal, A. A., Rebbapragada, U., Walters, R., et al. 2019, *PASP*, **131**, 038002
- Mahabal, A., Sheth, K., Gieseke, F., et al. 2017, arXiv:1709.06257
- Masci, F. J., Laher, R. R., Rebbapragada, U. D., et al. 2017, *PASP*, **129**, 014002
- Masci, F. J., Laher, R. R., Rusholme, B., et al. 2019, *PASP*, **131**, 018003
- Mauerhan, J., Van Dyk, S., & Wachter, S. 2012, *Photometric Monitoring of a New Sample of Candidate Luminous Blue Variables*, NOAO Proposal
- McCracken, H. J., Milvang-Jensen, B., Dunlop, J., et al. 2012, *A&A*, **544**, A156
- McCrum, M., Smartt, S. J., Rest, A., et al. 2015, *MNRAS*, **448**, 1206
- Meech, K. J., & Svoren, J. 2004, in *Comets II*, ed. M. C. Festou, H. U. Keller, & H. A. Weaver (Tucson, AZ: Univ. Arizona Press), 317
- Meech, K. J., Kleyana, J. T., Hainaut, O. R., et al. 2017, *ApJL*, **849**, L8
- Meegan, C., Lichti, G., Bhat, P. N., et al. 2009, *ApJ*, **702**, 791
- Mészáros, P., & Waxman, E. 2001, *PhRvL*, **87**, 171102
- Mooley, K. P., Nakar, E., Hotokezaka, K., et al. 2018, *Natur*, **554**, 207
- Moriya, T. J., Mazzali, P. A., Tominaga, N., et al. 2017, *MNRAS*, **466**, 2085
- Morozova, V., Piro, A. L., Renzo, M., et al. 2015, *ApJ*, **814**, 63
- Mulchaey, J. S., Kasliwal, M. M., & Kollmeier, J. A. 2014, *ApJL*, **780**, L34
- Murase, K., Oikonomou, F., & Petropoulou, M. 2018, *ApJ*, **865**, 124
- Murase, K., Thompson, T. A., Lacki, B. C., & Beacom, J. F. 2011, *PhRv*, **D84**, 043003
- Nadezhin, D. K. 1980, *Ap&SS*, **69**, 115
- Nakar, E. 2015, *ApJ*, **807**, 172
- Nakar, E., & Piran, T. 2018, *MNRAS*, **478**, 407
- Narayan, G., Zaidi, T., Soraisam, M. D., et al. 2018, *ApJS*, **236**, 9
- Naul, B., Bloom, J. S., Pérez, F., & van der Walt, S. 2018, *NatAs*, **2**, 151
- Nguyen, H.-L., Woon, Y.-K., & Ng, W.-K. 2015, *Knowledge and Information Systems*, **45**, 535
- Nicholl, M., Berger, E., Kasen, D., et al. 2017, *ApJL*, **848**, L18
- Nicholl, M., & Smartt, S. J. 2016, *MNRAS*, **457**, L79
- Nicholl, M., Smartt, S. J., Jerkstrand, A., et al. 2013, *Natur*, **502**, 346
- Nicholl, M., Smartt, S. J., Jerkstrand, A., et al. 2015, *ApJL*, **807**, L18
- Nordin, J., Aldering, G., Antilogus, P., et al. 2018, *A&A*, **614**, A71
- Nugent, P. E., Sullivan, M., Cenko, S. B., et al. 2011, *Natur*, **480**, 344
- Nyholm, A., Sollerman, J., Taddia, F., et al. 2017, *A&A*, **605**, A6
- Ofek, E. O., Cenko, S. B., Shaviv, N. J., et al. 2016, *ApJ*, **824**, 6
- Ofek, E. O., Lin, L., Kouveliotou, C., et al. 2013a, *ApJ*, **768**, 47
- Ofek, E. O., Rabinak, I., Neill, J. D., et al. 2010, *ApJ*, **724**, 1396
- Ofek, E. O., Sullivan, M., Cenko, S. B., et al. 2013b, *Natur*, **494**, 65
- Ofek, E. O., Sullivan, M., Shaviv, N. J., et al. 2014a, *ApJ*, **789**, 104
- Ofek, E. O., Zoglauer, A., Boggs, S. E., et al. 2014b, *ApJ*, **781**, 42
- Pastorello, A., Smartt, S. J., Mattila, S., et al. 2007, *Natur*, **447**, 829
- Patat, F., Taubenberger, S., Benetti, S., Pastorello, A., & Harutyunyan, A. 2011, *A&A*, **527**, L6
- Patterson, M. T., Bellm, E. C., Rusholme, B., et al. 2019, *PASP*, **131**, 018001
- Peng, F., Luo, Q., & Ni, L. M. 2017, in 2017 IEEE XXXIII International Conf. on Data Engineering (ICDE), 175
- Perets, H. B., Gal-Yam, A., Mazzali, P. A., et al. 2010, *Natur*, **465**, 322
- Perley, D. A., Quimby, R. M., Yan, L., et al. 2016, *ApJ*, **830**, 13
- Perlmutter, S., Aldering, G., Goldhaber, G., et al. 1999, *ApJ*, **517**, 565
- Phinney, E. S. 1989, in *IAU Symp. 136, The Center of the Galaxy*, ed. M. Morris (Dordrecht: Kluwer), 543
- Piro, A. L. 2013, *ApJL*, **768**, L14
- Planck Collaboration, Ade, P. A. R., Aghanim, N., et al. 2016, *A&A*, **594**, A13
- Prajs, S., Sullivan, M., Smith, M., et al. 2017, *MNRAS*, **464**, 3568
- Pravec, P., Vokrouhlický, D., Polishook, D., et al. 2010, *Natur*, **466**, 1085
- Prentice, S. J., Mazzali, P. A., Pian, E., et al. 2016, *MNRAS*, **458**, 2973
- Prialnik, D., Benkhoff, J., & Podolak, M. 2004, in *Comets II*, ed. M. C. Festou, H. U. Keller, & H. A. Weaver (Tucson, AZ: Univ. Arizona Press), 359

- Prieto, J. L., Brimacombe, J., Drake, A. J., & Howerton, S. 2013, *ApJ*, **763**, L27
- Quataert, E., & Shiode, J. 2012, *MNRAS*, **423**, L92
- Quimby, R. M., Yuan, F., Akerlof, C., & Wheeler, J. C. 2013, *MNRAS*, **431**, 912
- Raddi, R., Drew, J. E., Steeghs, D., et al. 2015, *MNRAS*, **446**, 274
- Rees, M. J. 1988, *Natur*, **333**, 523
- Rees, M. J., & Meszaros, P. 1992, *MNRAS*, **258**, 41P
- Refsdal, S. 1964, *MNRAS*, **128**, 307
- Ren, Y., Fox, E. B., & Bruce, A. 2017, *Ann. Appl. Stat.*, **11**, 808
- Rhoads, J. E. 1997, *ApJL*, **487**, L1
- Ribeiro, M. T., Singh, S., & Guestrin, C. 2016, in Proceedings of the XXII ACM SIGKDD Int. Conf. on Knowledge Discovery and Data Mining, ACM, 1135
- Riess, A. G., Casertano, S., Yuan, W., et al. 2018a, *ApJ*, **861**, 126
- Riess, A. G., Casertano, S., Yuan, W., et al. 2018b, *ApJ*, **855**, 136
- Riess, A. G., Filippenko, A. V., Challis, P., et al. 1998, *AJ*, **116**, 1009
- Riess, A. G., Macri, L. M., Hoffmann, S. L., et al. 2016, *ApJ*, **826**, 56
- Rigault, M., Brinnet, V., Aldering, G., et al. 2018, arXiv:1806.03849
- Rigault, M., Copin, Y., Aldering, G., et al. 2013, *A&A*, **560**, A66
- Rivinius, T., Carciofi, A. C., & Martayan, C. 2013, *A&ARv*, **21**, 69
- Roman, M., Hardin, D., Betoule, M., et al. 2018, *A&A*, **615**, A68
- Rubin, A., & Gal-Yam, A. 2017, *ApJ*, **848**, 8
- Rubin, A., Gal-Yam, A., De Cia, A., et al. 2016, *ApJ*, **820**, 33
- Saito, R. K., Hempel, M., Minniti, D., et al. 2012, *A&A*, **537**, A107
- Schlegel, E. M., & Petre, R. 2006, *ApJ*, **646**, 378
- Schulze, S., Krühler, T., Leloudas, G., et al. 2018, *MNRAS*, **473**, 1258
- Schutz, B. F. 1986, *Natur*, **323**, 310
- Schwamb, M. E., Jones, R. L., Chesley, S. R., et al. 2018, arXiv:1802.01783v1
- Scolnic, D. M., Jones, D. O., Rest, A., et al. 2018, *ApJ*, **859**, 101
- Sell, P. H., Maccarone, T. J., Kotak, R., Knigge, C., & Sand, D. J. 2015, *MNRAS*, **450**, 4198
- Senno, N., Murase, K., & Meszaros, P. 2016, *PhRvD*, **D93**, 083003
- Sesar, B., Ivezić, Ž., Lupton, R. H., et al. 2007, *AJ*, **134**, 2236
- Shappee, B. J., Prieto, J. L., Grupe, D., et al. 2014, *ApJ*, **788**, 48
- Shiode, J. H., & Quataert, E. 2014, *ApJ*, **780**, 96
- Singer, L. P., Price, L. R., Farr, B., et al. 2014, *ApJ*, **795**, 105
- Smartt, S. E. A. 2016, GCN, 19381, <https://gcn.gsfc.nasa.gov/gcn3/19381.gcn3>
- Smartt, S. J. 2015, *PASA*, **32**, 16
- Smartt, S. J., Eldridge, J. J., Crockett, R. M., & Maund, J. R. 2009, *MNRAS*, **395**, 1409
- Smith, M., Sullivan, M., D'Andrea, C. B., et al. 2016, *ApJL*, **818**, L8
- Smith, N., Kilpatrick, C. D., Mauerhan, J. C., et al. 2017, *MNRAS*, **466**, 3021
- Snodgrass, C., Tubiana, C., Vincent, J.-B., et al. 2010, *Natur*, **467**, 814
- Sobacchi, E., Granot, J., Bromberg, O., & Sormani, M. C. 2017, *MNRAS*, **472**, 616
- Soderberg, A. M., Berger, E., Page, K. L., et al. 2008, *Natur*, **453**, 469
- Soderberg, A. M., Kulkarni, S. R., Nakar, E., et al. 2006, *Natur*, **442**, 1014
- Sorokina, E., Blinnikov, S., Nomoto, K., Quimby, R., & Tolstov, A. 2016, *ApJ*, **829**, 17
- Soszyński, I., Stepień, K., Pilecki, B., et al. 2015, *AcA*, **65**, 39
- Soumagnac, M. T., Ofek, E. O., Gal-Yam, A., et al. 2019, *ApJ*, **872**, 141
- Stathakis, R. A., & Sadler, E. M. 1991, *MNRAS*, **250**, 786
- Stoll, R., Prieto, J. L., Stanek, K. Z., et al. 2011, *ApJ*, **730**, 34
- Stone, N., & Loeb, A. 2011, *MNRAS*, **412**, 75
- Stone, N. C., & Metzger, B. D. 2016, *MNRAS*, **455**, 859
- Stone, N. C., & van Velzen, S. 2016, *ApJL*, **825**, L14
- Strojtjohann, N. L., Ofek, E. O., Gal-Yam, A., et al. 2015, *ApJ*, **811**, 117
- Tachibana, Y., & Miller, A. A. 2018, *PASP*, **130**, 128001
- Taddia, F., Fremling, C., Sollerman, J., et al. 2016, *A&A*, **592**, A89
- Taddia, F., Sollerman, J., Fremling, C., et al. 2018a, *A&A*, **609**, A106
- Taddia, F., Sollerman, J., Leloudas, G., et al. 2015, *A&A*, **574**, A60
- Taddia, F., Stritzinger, M. D., Bersten, M., et al. 2018b, *A&A*, **609**, A136
- Tauris, T. M., Langer, N., Moriya, T. J., et al. 2013, *ApJL*, **778**, L23
- Tonry, J. L. 2011, *PASP*, **123**, 58
- Tonry, J. L., Denneau, L., Heinze, A. N., et al. 2018, *PASP*, **130**, 064505
- Tran, D., Kucukelbir, A., Dieng, A. B., et al. 2016, arXiv:1610.09787
- Troja, E., Piro, L., Ryan, G., et al. 2018, *MNRAS*, **478**, L18
- Turatto, M., Cappellaro, E., Danziger, I. J., et al. 1993, *MNRAS*, **262**, 128
- van Dyk, S. D., Weiler, K. W., Sramek, R. A., & Panagia, N. 1993, *ApJL*, **419**, L69
- van Eerten, H., Zhang, W., & MacFadyen, A. 2010, *ApJ*, **722**, 235
- van Velzen, S. 2018, *ApJ*, **852**, 72
- van Velzen, S., Farrar, G. R., Gezari, S., et al. 2011, *ApJ*, **741**, 73
- Vilalta, R., Ishida, E. E. O., Beck, R., et al. 2017, 2017 IEEE Symp. Series on Computational Intelligence (SSCI), 1
- Wang, J., & Merritt, D. 2004, *ApJ*, **600**, 149
- Wang, X., Smith, K., & Hyndman, R. 2006, *Data Mining and Knowledge Discovery*, **13**, 335
- Waszczak, A., Chang, C.-K., Ofek, E. O., et al. 2015, *AJ*, **150**, 75
- Waszczak, A., Ofek, E. O., Aharonson, O., et al. 2013, *MNRAS*, **433**, 3115
- Waszczak, A., Prince, T. A., Laher, R., et al. 2017, *PASP*, **129**, 034402
- Waxman, E., & Katz, B. 2017, in Handbook of Supernovae (Cham: Springer International), 967
- Whitesides, L., Lunnan, R., Kasliwal, M. M., et al. 2017, *ApJ*, **851**, 107
- Williams, C. L., Panagia, N., Van Dyk, S. D., et al. 2002, *ApJ*, **581**, 396
- Woosley, S. E. 2010, *ApJL*, **719**, L204
- Woosley, S. E., Blinnikov, S., & Heger, A. 2007, *Nature*, **450**, 390
- Yaron, O., Perley, D. A., Gal-Yam, A., et al. 2017, *NatPh*, **13**, 510
- Ye, Q.-Z. 2017, *AJ*, **153**, 207
- Ye, Q.-Z., Brown, P. G., Bell, C., et al. 2015, *ApJ*, **814**, 79
- Ye, Q.-Z., Hui, M.-T., Kracht, R., & Wiegert, P. A. 2014, *ApJ*, **796**, 83
- Yu, P.-C., Yu, C.-H., Lee, C.-D., et al. 2018, *AJ*, **155**, 91
- Zackay, B., Ofek, E. O., & Gal-Yam, A. 2016, *ApJ*, **830**, 27
- Zirakashvili, V. N., & Ptuskin, V. S. 2016, *Aph*, **78**, 28